Original Research

Impact of Silver-based Nanofluid on the Performance of Stepped Slope Single Basin Solar Still

Vikas Kumar [1], Dheerandra Singh [1,*], Virendra Kumar [1,*]

[1] Mechanical Engineering Department, Madan Mohan Malaviya University of Technology, Gorakhpur-273010, Uttar Pradesh, India.

* Correspondence: dsme@mmmut.ac.in (Dheerandra Singh); vkme@mmmut.ac.in (Virendra Kumar)

Received: February 18, 2026; Accepted: May 7, 2026

Abstract: Although solar desalination is a sustainable method of producing drinkable water, its poor productivity prevents it from being widely used. The current study combines geometric alteration with improved thermal energy storage and heat transfer to create a novel stepped-slope single basin solar still integrated with copper cylinders filled with silver-based nanofluid. Using mono nanofluids at various volume concentrations (0.01%, 0.03%, 0.05%, and 0.07%), the system's performance is experimentally examined and contrasted with a conventional solar still. To assess overall viability, a thorough 4E (energy, exergy, economic, and environmental) analysis is conducted. The optimum configuration with 0.07% silver nanofluid yields maximum energy efficiency (49.75%), exergy efficiency (3.46%), and freshwater productivity (2.81 kg/m²), according to the data. The suggested design also shows improved CO_2 mitigation, a shorter payback period, and lower costs. The results demonstrate the efficacy of combining stepped geometry with nanofluid-based heat storage, providing a viable and sustainable method for enhancing solar desalination systems and assisting clean water projects for sustainable development goals (SDG).

Keywords: solar energy; solar still; nanofluid; SDG; economic analysis; environmental analysis.

1. Introduction

Water is necessary for life and is utilized in many contexts, including agriculture, industry, and homes. And on the earth's crust, 95% of water availability is there in the form of ponds, glaciers, and the sea. But only 0.5% is used for drinking purposes, and the rest of the water found on the earth's surface is not used for drinking purposes. In other words, ensuring everyone has access to clean drinking water is one of the world's greatest problems. Due to excessive use of water resources for personal and commercial needs, groundwater supplies are running out. Surface water is more accessible, but a large portion of it is saline and unfit for human consumption. Moreover, the different conventional techniques, such as Reverse Osmosis, UV treatment, and Ozone treatment that convert saline water to potable drinking water consume electricity produced from burning of fossil fuels which are generally not sustainable and are responsible for major causes of environmental degradation, such as unpredicted climate changes, global warming, acid rain, and ozone depletion. Further, these techniques also require frequent periodic maintenance that increases the overall cost of operations and, hence, are not affordable to common people. Now, the solution to all such problems is the purification of saline water using the sun’s energy, also known as solar desalination. Solar desalination is a technique that utilizes the sun’s radiation to heat saline water, transforming it into water vapour, leaving the dissolved salts, and then condensing the vapour to fresh liquid water. The setups in which these processes are carried out are called Solar stills. Solar stills are classified into two types, namely, passive and active solar stills. In passive solar stills, the heating of saline water is done through sun’s radiation only without any aid of other external heating sources whereas, in active solar stills the heating of saline water takes place through sun's radiation along with use of various external heating sources such as solar collectors, PCM, nanofluids (NF), pebbles and gravels etc. This technique of water purification is very much sustainable, involves renewable energy sources, is less expensive, and is safer to the ecosystem [1, 2]. However, the productivity of fresh water from solar stills is quite low due to insufficient solar energy in the morning and evening hours, i.e., off-sunshine hours. Various research is being carried out to increase the performance of solar stills by employing different design modifications, heat storage materials such as stones and pebbles, HNFs, PCM, solar energy collectors, and reflecting surfaces.

Numerous studies on conventional solar stills have revealed certain drawbacks. By altering certain design characteristics, these restrictions can be eliminated. The impacts of different augmentations such as internal reflectors (IR), evacuated tubes, heat exchanger (HE), and external condenser (EC) on productivity and energy efficiency of Single slope solar stills was done by Bhargva and Yadav [1]. The authors have found that the overall energy efficiency and productivity were highest from SS employing (HE+IR+EC), having 33.6 %/206.5 % of energy efficiency and productivity, respectively, greater than conventional setups. However, the productivity from SS with (HE+IR) was also not less and is 203.5 % greater than conventional setups. Further, the authors have also discussed the augmentation of (ETC+HE) to SS, where the productivity was increased by 166.8 % higher to CSS, and when SS was integrated with (ETC+EC), the productivity was increased by 182.7 % higher than to CSS [1]. Abujazar et al. [2] have studied important parameters influencing the performance of solar desalination systems, which can be classified into climate, design, and operational aspects. Climatic factors encompass sun radiation, ambient temperature, and air velocity. Design elements encompass the evaporative and exposed surface areas, glazing cover material, angle, thickness, and materials utilized for the distiller and insulation. Operating parameters include water temperature, input water temperature, vacuum application, and temperature differentials [2]. Two distinct experimental sets were conducted on a south-facing single-slope solar still; the first set examined varied water depth levels (5, 6, and 7 cm) over many days by Al-Mezeini et al. [3]. The findings indicated that the solar still with a water depth of 4 cm had attained the highest productivity/efficiency of 2.680 l/day/30%, respectively, in contrast to depths of 5, 6, and 7 cm. Second, when an external mirror was incorporated into the single slope, it resulted in an elevation of the basin's temperature, which enhanced the water productivity from 2.680 l/day to 3.075 l/day and hence improved the efficiency from 30 to 35% [3]. Hemispherical solar stills were investigated by Attia et al. [4] by incorporating black Cu,Zn and Fe trays at the basin bottom to enhance heat transfer and evaporation performance solar still. The studies revealed that the traditional hemispherical solar still (CHSS) generated 4.8 $kg/m^2/day$, whereas modified designs yielded high yields of 5.5, 6.3, and 7.35 $kg/m^2/day$ for iron, zinc, and copper pans. Iron production increased 17%, zinc 31.25%, and copper 53.125% above CHSS [4]. investigations of performance parameters and also compared the results with CSS. The authors obtained results to show maximum productivity was 11.1 l/m^2 from MSS and 2.88 l/m^2 from CSS, with an increase of 286 % to 300 % in the summer season [5]. An investigation was presented by Gholizadeh and Farzi [6] on the use of sand as thermal energy storage in a SSSS to enhance its performance. The authors have experimented on SSSS with and without use of sand at basin at Iran. The authors' results show an increment of 21.43% in thermal efficiency and productivity when compared to CSS. In addition, the authors have also discussed the effects of wind speed on the performance of SS [6]. Miqdam Tariq Chaichan et al. [7] examined a solar still by implementing cooling methods such as fan cooling and water cooling of the glass cover to mitigated the issue of elevated glass cover temperatures. The author's findings indicated that the proposed design enhanced productivity by 120.8% without cooling, while productivity further escalated by 337.36% with fan cooling and 403% with water cooling [7].

To increase the working period of solar stills, some energy storing materials can be used which can increase the performance by making the apparatus effective during off sunshine periods and non-availability of sun rays in daytime. These materials may exhibit sensible or latent heat transfer. Because of their superior thermodynamic qualities, PCMs are frequently used as latent heat transfer type heat storage materials. Al-harahsheh et al. [8] have studied the performance of a solar still equipped with solar collector and phase change material (PCM) (as Sodium Thiosulfate Pentahydrate) experimentally. Further, they also investigated the impact of basin water level, cooling water flow rate, and hot water circulation flow rate on freshwater production. The authors have found that the productivity of the unit was increased using solar collectors and PCM, as both have added the energy (sensible and latent) and have maintained the setup running continually (i.e., operating day and night). The highest yield productivity from the setup was 4300 ml/m^2 per day, out of which 40% of the productivity, i.e., 1720 ml/m^2, was obtained after sunset [8]. Ramzy et al. [9] have used various natural and synthetic absorbent materials, such as steel wool pads, fine steel wool, and black luffa at the still basin, and analyzed the performance of solar stills. According to the experimental results, solar stills employing steel wool pads had the highest yield production of 4.384 l/m^2 and a maximum thermal efficiency of 32.74%. Besides, Steel wool pads had the cheapest price per liter, at \$0.0034/l/m^2, and hence are more economical than other absorbent materials. Another experimental investigation on a modified solar still (MSS) and conventional solar still (CSS), comparing distillate output, energy efficiency, and cost of distillate produced under the same climate [9]. Alasiri and Shanmugan [10] investigated the M-shaped absorber plate SSSS using Mn_2O_3-doped Cu nanocomposite and Paraffin RT31 over winter and summer seasons. This design, using aluminium cans, attained superior performance, increasing daily freshwater yield by 25.4% compared to traditional stills. Winter yield rose from 3.45 to 6.32 kg/m^2, and summer yield ascended from 2.953 to 6.594 kg/m^2. Thermal efficiency increased from 32.9% (CSS) to 42.7% [10]. Vijayakumar and Karthick [11] examined a double-slope solar still (DSS) using phase change materials (PCMs) augmented with Graphene Oxide (GO) nanoparticles and Glauber's salt. The author's results show that the GO–salt nano-PCM attained the maximum production of 2751 ml/day, increasing productivity by 63.07%, 23.36%, and 12.65% compared to the other instances. The system achieved maximum energy and exergy efficiencies of 43.06% and 2.47%, respectively, and the greatest evaporative heat transfer rate of 91.25 W/m^{2}K[11] .Shajahan et al. [12] conducted experiments on double-slope solar stills (DSS) at three distinct water depths (2 cm, 5 cm, and 7 cm) with three design modifications: a conventional DSS without PCM, a DSS with encapsulated PCM placed in an aluminium box at the basin, and a DSS with nano-enhanced PCM, which was doped with 25 wt% silver nanoparticles, encapsulated, and place in the basin. The experiments were carried out for 24 hours from 6:00 a.m. to the next day at 6:00 a.m., and the results were compared. The author's results show the simple DSS had a maximum efficiency of 20.52% at 2cm depth. Further, the results also show that the incorporation of the PCM and nano-enhanced has reduced efficiency for the first nine hours from 06:00 am, as the PCM absorbs some of the heat energy. However, after the sunsets, the stored energy is returned from PCM to Saline water. The maximum/minimum efficiency for the second modification was 33.43 %/18.55%, and for the third modification was 35.3%/25.62% at 2cm and 7cm, respectively [12]. By combining various heat storage materials, it has been suggested by Karthikeyan et al. [13] that solar desalination systems' performance (yield and energy efficiency) can be enhanced. Using a variety of sensible heat storage medium, including glass balls, gravel, pebbles, nanomaterials (Al_2O_3), and black dye, the research was investigated on single-slope solar stills (SSSS) which show that the setup using Al_2O_3 as energy storage material has higher yield production than any other heat energy storage materials as nano-materials have higher absorption and storage of solar energy. In addition, the results also show that the performance of SS depends upon the depth of basin water, slope inclination, and energy storage materials [13]. In order to enhance water productivity in a double-slope solar still, Gupta and Solanki [14] investigated the performance by the use of steel wool fibre as wick material, eutectic PCM (Myristic acid + Stearic acid), and nano-enhanced PCM with Ag_2O_3 nanoparticles. Four configurations were put to the test: CSS (without PCM), DSS-1 (with eutectic PCM), DSS-2 (with eutectic PCM and steel wool), and DSS-3 (with nano-enhanced eutectic PCM). DSS-3's cumulative freshwater yield was 4.22 kg/m², which was 132%, 72.9%, and 24.1% greater than that of CSS (1.82 kg/m²), DSS-1 (2.44 kg/m²), and DSS-2 (3.40 kg/m²). Additionally, DSS-3 outperformed CSS by 45.9%, DSS-1 by 32.8%, and DSS-2 by 6.1% in terms of total heat transmission. In contrast to CSS (22.21%), DSS-1 (30.42%), and DSS-2 (41%), DSS-3 had an average energy efficiency of 49% with a 12.2% energy efficiency [14]. A study was conducted by Hafs et al. [15] to examine the seasonal thermal performance of a modified single-slope solar still (MSSRC) that was configured with rectangular channels that were filled with heat storage material. In order to optimise the number and diameter of the channels, parametric analysis was conducted numerically using the Finite Element Method (COMSOL Multiphysics). Five channels, each measuring 2 cm in width, were determined to be the most effective design, as it was consistent throughout all seasons. According to the findings, the modified still has the ability to increase daily productivity by 24.40% during the autumn season, 37.79% during the winter season, 9.80% during the spring season, and 22.66% during the summer season when compared to normal solar still [15].A Solar still hollow-finned absorber basin (SSHF) with and without paraffin wax PCM (SSHFP) was employed by Suraparaju et al. [16] to conduct an investigation. The efficacy of CSS was compared to that of a SSHF and a hollow-finned absorber basin embedded in polymer composite material (SSHFP). According to the experimental findings, SSHF was able to raise yield by 15.7%, while SSHFP has increased productivity by 52.4% in comparison to CSS [16]. Poonia et al. [17] have examined a dish concentrator-based solar desalination system that uses paraffin wax as PCM to heat water and boost production in off-sunshine hours at ICAR Jhodhpur. The author's results revealed that for year-round analysis, the PCM has raised the daily yield production from 6.52 l to 7.12 l in May 2020. However, the average monthly distillate yield rose from 3.84 l to 4.51 l upon the use of PCM. Overall, the integration of PCM to dish concentrator solar desalination has increased productivity by 109% [17]. An experimental investigation was conducted by Kumaravel et al. [18] to assess the performance of a CSS by incorporating phase change material (PCM) or marble stones as thermal energy storage media in order to improve productivity and efficiency. The results show that the solar still using PCM produced 4820 ml/m² of desalinated water, whereas SS with marble stone-based still produced 5492 ml/m^2. PCM and marble stones boosted productivity by 26% and 41%, respectively, over a traditional solar still. Marble-supported stills were more efficient during the day, but PCM-supported stills were better at night. The marble stone-based still had 63% daily efficacy, while the PCM-based still had only 53% efficiency [18]. An experimental study was conducted by Suraparaju and Natarajan [19] to enhanced the efficiency of SSSS by using natural fibres. The efficiency of CSS with and without natural fibres was analysed and compared, and ridge gourd fibre was incorporated into a modified CSS due to its high porosity and simple availability. The experimental results show that the use of ridge gourd has decreased the yield and energy performance compared to CSS and hence has no significance on using such natural fiber [19]. The effectiveness of DSS in processing high-TDS water under six distinct configurations was examined by Kumbhar [20]. The instances comprised variants utilising brackish water or RO wastewater, as well as variations with and without reflectors and PCM: DSS with reflectors and PCM (brackish water) is the first case; DSSS with reflectors and PCM (RO wastewater) is the second; DSS with reflectors and PCM (brackish water) is the third; DSS with reflectors without PCM is the fourth; DSS with reflectors and PCM is the fifth; DSS with reflectors and PCM is the sixth; and DSS with reflectors and PCM is the sixth case. The author results show the maximum efficiency/distillate output for Case 6 as 42.10%/1610 ml and minimum efficiency/productivity for Case 1 as 26.1%/1070 ml, respectively [20]. A comparative study was conducted by

Kouravand et al. [21] to improve the efficiency of double-slope solar stills (DSS) by testing five distinct configurations: Setup 1 is a simple DSS. Setup 2: DSS is insulated with rock wool. Setup 3: DSS is integrated with an aluminium plate at the basin absorber. Setup 4: DSS is integrated with PCM (hydrated minerals) in copper tubing at the basin. Setup 5: DSS is integrated with insulation, PCM, and an aluminium plate at the basin. The results reveal the average efficiency/productivity per day as 45.2%/385ml (maximum), 40.5%,353ml, 36.6 %/320ml, 36.1%/314ml, and 33.1%/271ml (minimum) for Setup 5, Setup 2, Setup 3, Setup 4 and Setup 1, respectively [21]. The mass of PCM (stearic acid) was changed by El-Sebaii et al. [22] throughout the summer and winter months in Saudi Arabia in order to perform an assessment on the daytime, nighttime, and overall daily production and efficiency of a single-slope, single-basin solar still. The results tell that as the mass of PCM increases, the daytime productivity decreases, however the nighttime and daily yield productivity increases with increased mass.Further, on summer days, the still with PCM produced 9.005 kg/m² with 85.3% efficiency, compared to 4.998 kg/m² without PCM [22]. An experiment was conducted by Tuly et al. [23] with the purpose of enhancing the production of drinkable water from active DSS by using a combination of solid rectangular fins, paraffin wax, black cotton fabric as thermal storage, and an external condenser (Setup 1). There was also a comparison made between the performance of a conventional DSS (Setup 2) and a DSS that had been modified with rectangular fins (Setup 3). The author's experimental results show the maximum productivity of 3.07 l/m^2 was from Setup 1, then from Setup 3 with 2.70 l/m^2, and Setup 2 with 2.46 l/m^2. Moreover, the average daily efficiency of Setup 1 is higher by 14.23 % and 22.23 % when compared to Setup 3 and Setup 1, respectively. Further, economic analysis showed traditional, finned, and modified stills cost $0.0135, $0.0133, and $0.0117 per liter [23]. An investigation was conducted by Faegh and Shafii [24] on a solar still with an external PCM-filled condenser. The entire setup generated 6.555 kg/m²/day yield with 50% efficiency, an 86% increase over the traditional design [24]. A theoretical model of a SSSS using PCM for energy storage was introduced by Mousa and Gujarathi [25] through examine the impact of PCM variables including amount, melting point, and solar radiation on system efficacy. The authors results conclude that productivity increases as melting point of PCM increases, solar radiation increases but show negative results with an increase in the mass of PCM [25]. Damene et al. [26] conducted an experimental investigation of a solar water heating system utilizing phase change material (PCM) masses of 0.5 kg and 1 kg. The author's findings indicate that the PCM-assisted system maintained water temperatures exceeding 52 °C for nearly four additional hours owing to latent heat storage [26].

The usefulness of PCMs can be increased by mixing particular nanoparticles in different concentrations with PCMs; this is referred to as nano-enhanced PCMs. Authors' experimental results show that MSS employing heating coil only results in increase of 76 %/45.4 % higher productivity and thermal efficiency, respectively, than CSS, MSS with copper heating coil of and internal reflectors at the back wall have an increase in productivity by 92%, MSS utilizing heating coil, internal reflectors, and external reflectors have enhanced the productivity and thermal efficiency higher by 134%/54.1%, respectively [27]. Benghanem et al. [28] examined solar distiller configurations utilising a copper heat coil with solar collector and coating of silver (Case-1), incorporating silver nano-enhanced PCM beneath the absorber surface (Case-2), and adding reflectors alongside the previous modifications (Case-3). The most effective result was recorded in Case-3, producing 11.66 l/m² with a 228.45% enhancement compared to conventional stills. It attained the maximum thermal efficiency of 62.29% and exergy efficiency of 191.16%, decreased freshwater costs by 48.22%, and reduced CO_2 emissions by 47.81 tons [28]. Sathyamurthy [29] used doping of silver (Ag) nanoparticles (at 1 and 2% by weight) in paraffin wax and only using paraffin wax. The authors experimental work reveals that upon utilizing nano-enhanced PCM or simply PCM the water temperature, evaporation rate, and accumulated potable water were higher in the case of solar still (SS) using nano-enhanced PCM (i.e., 7.98kg/m^2 day), followed by only PCM (i.e., 6.73 kg/m^2 day), and then without using any energy storage materials (i.e., 3.61 kg/m^2 day). Further, the economic analysis presents that the cost per liter of fresh water was higher in the case of SS using nano-enhanced PCM and only PCM than SS with no energy storage materials, i.e., conventional setups. However, the yearly productivity of fresh water was increased in the case of SS employing nano-enhanced PCM by 18.42 % and 120.72 % when compared to SS using only PCM and SS without any energy storage materials, respectively [29].

Various researches have done their work on solar stills using sensible heat storage materials, mostly, nanofluids of different concentrations on base fluid to increase the performance. Miqdam T. Chaichan et al. [30] examined a nanofluid incorporating multi-walled carbon nanotubes (MWCNTs) to enhance thermal properties and stability in a photovoltaic/thermal (PVT) system utilizing CTAB, SDS, and SDBS. The ideal formulation consisted of 0.5% MWCNTs dispersed in water with CTAB as the surfactant, yielding superior thermal conductivity and stability compared to ethylene glycol, propylene glycol, and oil-based fluids. the author results show that the MWCNT nanofluid-cooled PVT system enhanced electrical efficiency by 88.85% relative to standalone PV and by 44% compared to water-cooled PVT, while thermal efficiency increased by 20% [30]. Kumar et al. [31] experimented on SSSS having external reflectors and hybrid NFs. Authors found that there was 29.84% incremental growth in distillate output for single-slope solar still (SSSS) using NFs as compared to that without using [31]. Sahu and Tiwari [32] studied the effects on performance of SSSS using different nanofluids (SiO_2, Al_2O_3, hybrid NFs SiO_2+Al_2O_3) in the winter season. The author's experimental results show that setup utilizing nanofluids of Al_2O_3 have maximum productivity of 670ml/m^2 day and energy efficiency of 30.27 %, followed by setups with hybrid NF's (SiO_2+Al_2O_3) having productivity 610 ml/m2 day and efficiency of 26.81%, followed by setup using SiO_2 nanofluids with productivity of 550ml/m^2 day and energy efficiency of 23.14% [32]. Singh et al. [33] have reviewed different aspects of various hybrid and mono nanofluids (NF), such as properties, preparation, stability, different ways to enhance stability, and their applications in solar desalination systems. The authors have also highlighted the different significant properties of different hybrid nanofluids and their uses as heat transfer and energy storage materials by different researchers in solar desalination systems [33]. Some widely used nanoparticles (such as Al_2O_3, CuO, TiO_2, MWCNT, Ag, SiC, and SiO_2) have been discussed by Gajbhiye et al. [34] in solar desalination systems for productivity enhancement. The authors have also discussed the effects on freshwater productivity by varying concentrations of nanoparticles in nanofluids. According to the author's results, productivity increased as the percentage of nanoparticles increased. The authors also highlighted the significance of SiC nanoparticles in solar desalination systems, as SiC has low luminosity, high thermal conductivity, and low cost [34]. The optical and thermal properties of commonly used NFs, along with their applications in solar desalination systems and the optimization of various forms, have been extensively investigated by Isravel and Karunamurthy [35]. In addition, the authors have also looked at how nanofluids have affected the production of distillate, evaporation rate, and heat absorption, in solar still operation. The author's comprehensive investigation showed that using NFs in solar still basins enhance the thermal conductivity and optical characteristics of the base fluid, which raises the temperature difference between the evaporation and condensation zones, nanofluids, and, thus, boosts the productivity of solar stills. In addition, the authors have also suggested that in order to maintain freshwater production, nanofluid stability is essential since inadequate dispersion of nanoparticles might result in agglomeration and decreased efficiency [35]. The performance of three types of similar SS was tested and compared by Parsa et al. [36] by adding three different modifications: a thermoelectric heating device (TEH) with nanofluids (NFs) for heating and a water film and thermoelectric condenser (TEC) for cooling. In the first modification, SS was integrated with a TEH device in the basin only, while the second modification was SS coupled with TEH and NFs simultaneously, and the third modification in SS consisted of TEH, NFs, and TEC simultaneously. The author's experimental results revealed that SS modified with TEH, NFs, and TEC have the highest daily yield and efficiency. And upon comparison to SS with TEH only (i.e., without NF's and TEC), this increase was 100.5%/26.7 %, respectively. When SS with TEC, NFs (i.e., without TEC) were compared with SS having TEH, only the increase in daily yield/efficiency was 50.8%/30.8%, respectively. The authors also have revealed that integrating external condensers contributes 26.3% to overall production [36]. An experimental investigation was undertaken by Zakaria et al. [37] to assess the efficiency of flat-plate and evacuated-tube collectors for water distillation in outdoor environments, with close monitoring of sun intensity, water mass flow rate, and temperature.The evaporation efficiency of the flat-plate collector was enhanced by as much as 36% when ethylene glycol nanofluid was employed at temperatures ranging from 80 to 100°C [37]. Sathish et al. [38] investigated an HDH desalination system integrated with an evacuated tube solar collector (ETSC) and a flat air collector (FAC). The author uses a hybrid MWCNT/TiO_2 nanofluid (0.1% each) in ETSC and nano-enhanced coating in FAC to improve the heat transmission and absorption. The author results show that the hybrid nanofluid reached 73.4°C, 324.6W heat input, and 67.3% humidifier efficiency. Water productivity increased to 799.7 mm^3/h with nanofluid and 806.4 mm^3/h with nanocoating [38]. Patel et al. [39] examined the square pyramid solar still using mono (Cu, Al_2O_3) and hybrid (Al_2O_3–Cu) nanofluids at a concentration of 0.1 wt%. The results indicated that Cu nanofluid outperformed Al_2O_3, achieving a productivity of 1640 ml/m² and an efficiency of 17%. The hybrid Al_2O_3–Cu nanofluid succeeded both mono-nanofluids, with 20:80 ratio (Al_2O_3–Cu) achieving the greatest output of 2644 ml/m² and an efficiency of 34.5% [39]. A study was performed by El-Gazar et al. [40] to see how well a mixed nanofluid improved the performance of CSS in the climate of Egypt. The authors have used a HNF of (Al_2O_3+CuO) at a concentration of 0.025% to modify stills and compared the results with CSS. The study results show that NF raises the yield productivity by 5.539 kg/m^2 and 3.1079 kg/m^2 in summer and winter, with an enhancement of 27.2% and 21.7% in summer and winter seasons, respectively when compared to CSS [40]. Sai et al. [41] examined DSS using ZnO nanofluids derived from sugarcane juice (SNZ) at concentrations of (10%, 20%, and 40%) by spray pyrolysis. SZN at the ideal 30% concentration demonstrated increased stability, superior heat transmission, and synergistic interactions from sugarcane juice constituents. The revised DSS attained an average distillate output of 3.5 kg/day using SZNs [41]. An experimental study was carried out by Kandasamy et al. [42] to enhance the thermal performance of solar collectors using silver nanoparticle-based nanofluids. The authors have tested to optimize the thermal performance for different size of silver nanoparticles (from 20 nm to 50 nm) and also at different concentrations (say from 0.2 wt % to 0.8 wt %).The authors studies show that nano-particles at smaller sizes i.e., 20 nm at lower concentration of 0.2 wt % yield the maximum thermal conductivity of 0.73W/mK because of high surface area to volume ratio [42]. Rasaiah et al. [43] investigated conventional and modified double-slope solar stills (DSS) employing ZnO, Al_2O_3, and CuO nanofluids (0.1 vol.%) and solar-actuated vacuum fan with external condenser. CuO nanofluid increased distillate production by 75.86% over conventional stills. CuO had peak energy and exergy efficiencies of 28.37% and 57.07%. In addition, CuO offered the maximum CO_2 mitigation (16.80 tonnes) and carbon credits ($504.09) [43]. The efficiency of drinkable water production was evaluated by Prasad et al. [44] for single-slope (SSl) and square-pyramid (SPy) solar stills, both with and without phase change material (PCM), across four configurations: Setup 1 – CSS, Setup 2 – SPy SS, Setup 3 – CSS with paraffin wax PCM, and Setup 4 – SPy SS with paraffin wax. The experimental results show that PCM variants of CSS and Spy SS produced 18.71% and 21.11 % higher productivity than simple SSl and Spy [44]. Harby et al. [45] studied the conventional and modified hemispherical solar still incorporating stainless-steel and aluminum shavings along with CuO nanofluid (0.05 wt%). The author's results indicate that the aluminum-based system attained the highest freshwater productivity of 8.87 L m^{-2} day^{-1}, reflecting a 115.6% enhancement compared to the conventional still. Furthermore, energy efficiency attained 48.7% and exergy efficiency reached 2.71%, indicating enhanced thermal and thermodynamic performance [45]. Elango et al. [46] investigated single and double-basin glass solar stills with a basin area of 0.81 m^2 under insulated conditions, utilizing saline borewell water and nanofluids (SnO_2 and ZnO and Al_2O_3) at a water depth of 1 cm to facilitate evaporation. The author results show that the double-basin still utilizing Al_2O_3 nanofluid attained the maximum productivity of 5405 mL/m^2/day, surpassing both water and SnO_2 and ZnO nanofluids [46].

After a thorough analysis of the literature, it is found that while considerable efforts have been made to improve solar still performance through design changes, nanofluids, and thermal energy storage materials, very few studies have concentrated on the combined use of stepped basin geometry with sensible heat storage based on nanofluids. Specifically, there is still much to explore regarding the integration of silver-based nanofluids into copper cylindrical storage elements in a stepped-slope single-basin solar still. Although Sathyamurthy [29] examined the characterization of silver nanoparticles incorporated in paraffin wax as a latent heat storage medium in a stepped (basin) solar still, and evaluated its thermal performance, economic aspects, and water quality, the analysis remains limited. There is further scope to investigate additional performance metrics, such as exergy and environmental impacts, for a more comprehensive assessment of the stepped solar still. Therefore, the novelty of this study lies in the design and experimental evaluation of a stepped-slope (transparent glass) solar still integrated with copper cylinders containing silver nanofluid to simultaneously enhance heat transfer, thermal storage, and freshwater productivity. Furthermore, the work identifies the optimal nanofluid concentration and provides a comprehensive 4E (energy, exergy, economic, and environmental) comparison with a conventional solar still based on different configurations.

2. Experimental setup and methodology

The experimental setups consist of a conventional solar still (CSS) and a modified configuration featuring a single basin with a three-stepped slope designed for enhanced heat transmission and water collection, referred to as a Stepped solar still. Figures 1 (a) and 1 (b) present the schematic and line diagrams of the CSS, while Figures 2 (a) and 2 (b) illustrate the schematic and line diagrams of the stepped solar still. Both setups featured identical basin dimensions of 1 m x 1 m, coated with black paint to maximize solar radiation absorption. The slope angle was 26.7°, corresponding to the latitude of Gorakhpur, Uttar Pradesh, facilitating optimal solar radiation capture. The glass cover had a thickness of 3 mm, with front and back heights of 0.16 m and 0.97 m, respectively, and an inclined height of 1.10 m. The construction utilized GI sheets with a thickness of 0.6 mm. The modified setup incorporates eight covered cylindrical copper pipes, each with a diameter of 0.07 m and a height of 0.035 m, welded to the basin for the storage of nanofluids prepared at varying concentrations.. The side walls of the SS were insulated with thermocol of thickness 0.02 m to prevent any heat losses from the system to the surroundings. The arrangements for the different setups goes like, conventional single slope CSS (**Setup 1**), modified still with stepped wise slope single with single basin (MSWSSSB) (**Setup 2**), MSWSSSB filled with silver nanofluid inside copper cylindrical pipe prepared at a volume concentration of 0.01% (**Setup 3**), MSWSSSB filled with silver nanofluid inside copper cylindrical pipe shape at volume concentration of 0.03% (**Setup 4**), MSWSSSB filled with silver nanofluid inside copper cylindrical shape having at volume concentration of 0.05% (**Setup 5**), MSWSSSB filled with silver nanofluid inside copper cylindrical shape at volume concentration of 0.07% (**Setup 6**).

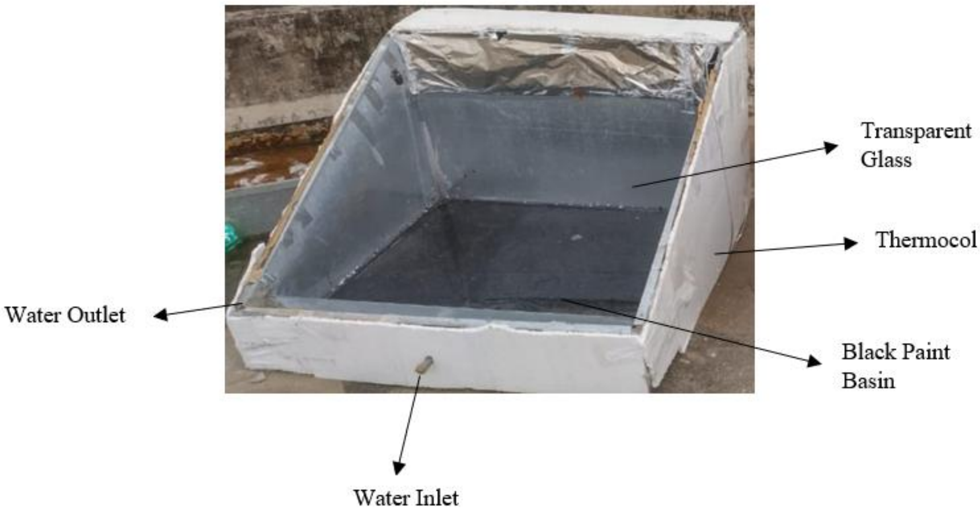

Figure 1(a). Schematic view of the experimental setup of the conventional solar still.

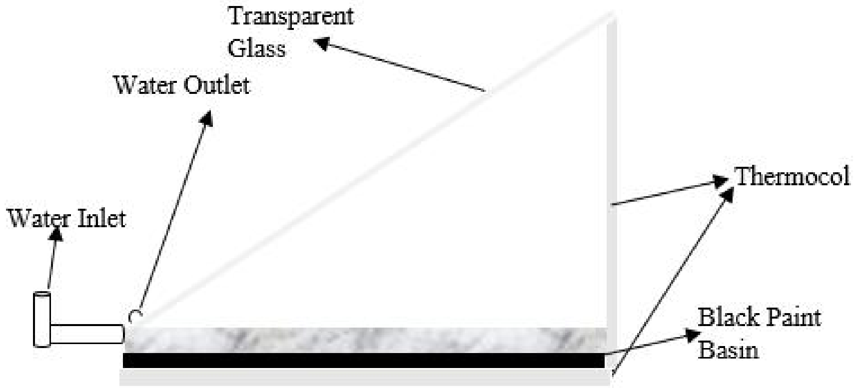

Figure 1(b). Line diagram of the side view of the conventional solar still.

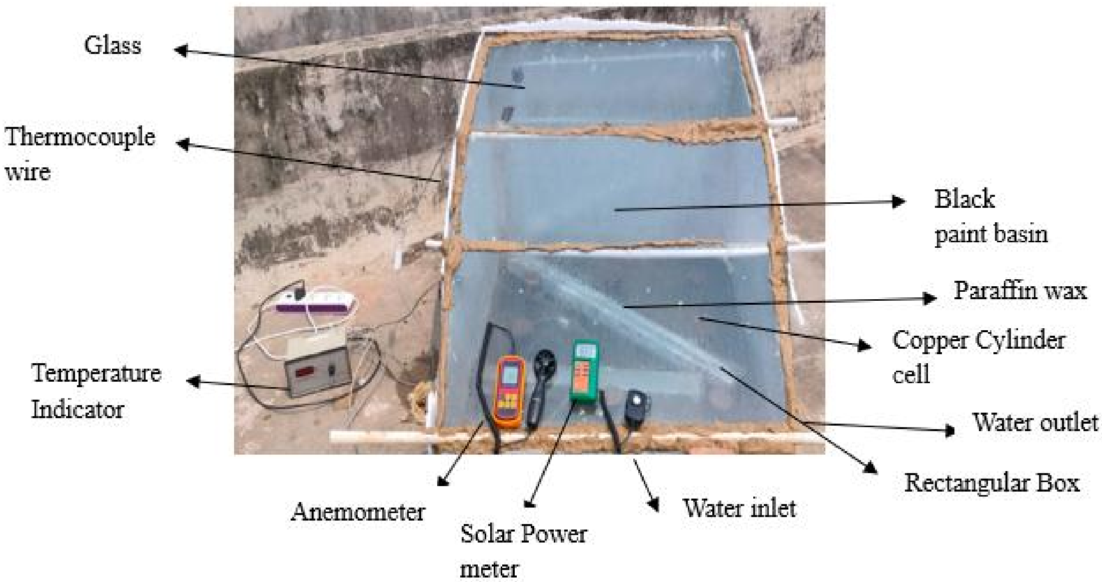

Figure 2(a). Schematic view of the experimental setup of the stepped solar still.

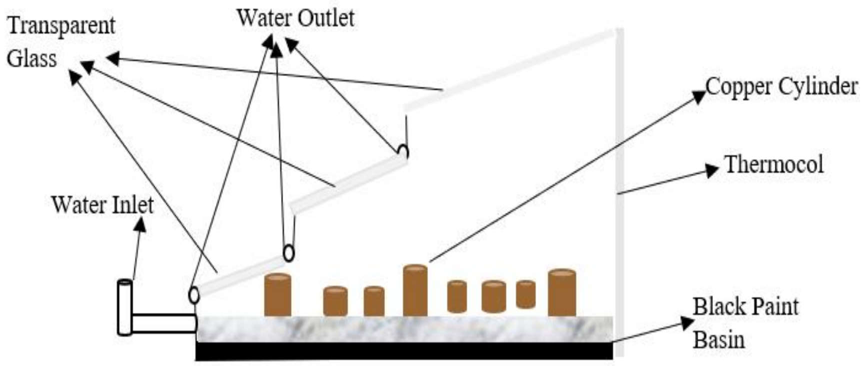

Figure 2(b). Line diagram of the side view of the stepped solar still.

The main aim of current study is to examine the performance of experimental setup in the season of lower input energy, i.e., the winter season. Therefore, the experimental work was conducted on the roof of the Mechanical Engineering Department at MMMUT Gorakhpur, situated at Latitude 26.76°N and Longitude 83.37°E during the winter season in October. This study examines the performance of solar stills across various configurations, specifically Setup 1, Setup 2, Setup 3, Setup 4, Setup 5, and Setup 6 in six consecutive days. A constant water depth of 2 cm was maintained across all arrangements. Additionally, all varied configurations were oriented towards the south to optimize solar radiation absorption. The variation in environmental factors, including solar intensity, ambient temperature, wind velocity, and temperature at various locations and arrangements, was measured at 30-minute intervals from morning until 7:00 a.m. the following day, covering a total duration of 24 hours. Each variation was measured twice to ensure the correctness and accuracy of the results which were presented through error bars in each graphs.

2.1. Preparation of nanofluid

Nanofluid is defined as a colloidal suspension of nanoparticles, ranging from 1 nm to 100 nm, uniformly dispersed in a base fluid, which may include water, oil, ethylene glycol, or their combinations. Its superior thermo-physical properties, including heat transfer coefficients, viscosity, thermal conductivity, and thermal diffusivity relative to base fluids, demonstrate its extensive applicability in heat transfer applications. Furthermore, it has attracted the interest of numerous researchers in recent years regarding heat transfer applications, including heat exchangers and solar collectors [47]. The silver nanoparticles utilized in this study were obtained from Adnano Technologies Private Limited. The provided silver nanoparticle exhibited a purity of 99.9%, an average particle size of 80–100 nm, and a specific surface area (SSA) of 3–5 m^2/g. The substance possesses a molecular formula of Ag, a molecular weight of 107.87 g/mol, a melting point of 960.8 °C, a bulk density of 1.2 g/cm^3, and a CAS number of 7440-22-4.

The synthesis of silver-based nanofluids at diverse volume concentrations of 0.01%, 0.03%, 0.05%, and 0.07%, utilizing the recognized two-step method using base fluid as deionosed water [48]. In this method, the weight of silver nanoparticles are measured using a weighing machine and subsequently gradually dispersed into the base fluid. The mass of silver nanoparticles at different volume concentrations was calculated from the Eqn. (1)

$$\varphi = \left[\frac{\left(\frac{M}{\rho}\right)Ag}{\left(\frac{M}{\rho}\right)Ag+\left(\frac{M}{\rho}\right)Base\ fluid}\right] \quad (1)$$

In order to produce stable homogenous silver NFs at various volume concentrations, the same amount was measured using electronic weighing scales and then dispersed to the base fluid (i.e., deionized water) of the required volume. The colloidal solutions were then exposed to a magnetic stirrer for three hours at a speed of 850 rpm and a temperature of 60 °C, followed by an ultrasonic probe sonicator for thirty minutes to prevent agglomeration and sedimentation brought on by the strong Van der Waals force of attraction. The schematic steps for preparation of the nanofluid are given in Figure 3.

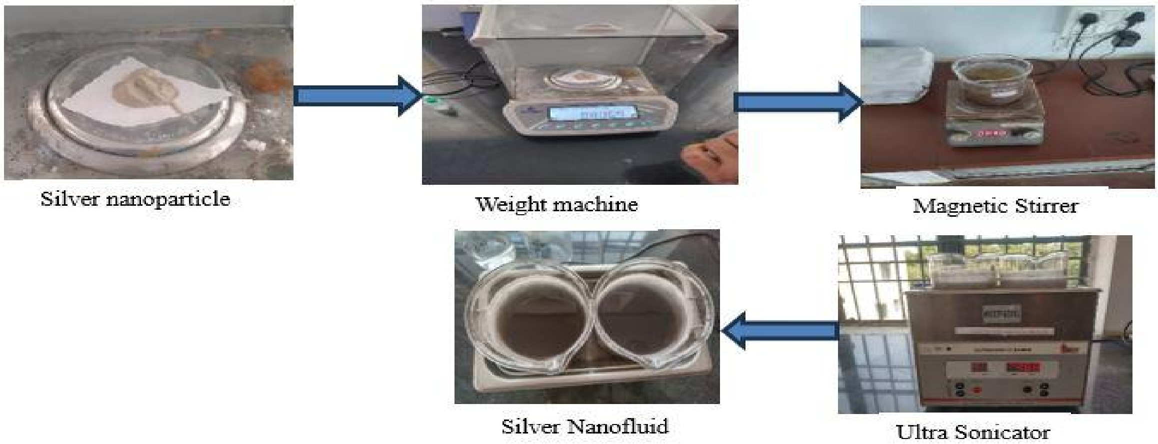

Figure 3. Preparation of silver nano-fluids.

2.2. Instrumentation and accuracy

The various instruments used for measuring the variation in environmental parameters, i.e., solar radiation intensity, wind velocity, and ambient temperature, were: Solar Power Meter (TENMARS TM-207) for radiation intensity, Anemometer (KM 908 MK1) for wind velocity, and thermometer for ambient temperature. In addition, due to variations in environmental parameters with respect to day time, the variation in temperatures at different locations such as inner glass, water, basin, NFs, and PCM inside the SS setups were measured using different K type thermocouple wire whose one end is connected to location of which we want to measure the temperature and other end is connected to multi point temperature indicator device (TI12), that indicates the temperature of particular locations. The half-hourly yield productivity from SS is measured using a cylindrical flask. However, the uncertainty in the measurement of different parameters through different instruments was obtained from the following equation [19] and are given in Table 1.

$$u = \frac{a}{\sqrt{3}}$$

Table 1. Technical specifications of measuring devices.

Instrument	Accuracy	Range	Uncertainty
K-type thermocouple	± 0.1 °C	0–200 °C	0.05 °C
Digital multi point temperature indicator	± 1 °C	0–200 °C	0.5 °C
Solar Power Meter	±10 W/m^2	0-1999 W/m^2	5.7 W/m^2
Anemometer	± 0.1 m/s	0.2-20 m/s	0.05 m/s
Measuring Flask	± 1 ml	0-1000 ml	0.5 ml

In order to monitor temperature at all times of the day, K-type thermocouples are calibrated. It was employed for data reading and recording. Throughout the working period, temperature, production of distilled water, and other parameters were measured. With these data, the uncertainty values are computed.

$$v = f(n_1, n_2, n_3 \dots\dots n_m)$$

The resulting uncertainties (U) were estimated for uncertainty values of m_1, m_2, … in the independent variables n_1, n_2, … as given in Eqn. 2.

$$U = \sqrt{\left(\frac{\partial v}{\partial n_1} m_1\right)^2 + \left(\frac{\partial v}{\partial n_2} m_2\right)^2 + \left(\frac{\partial v}{\partial n_3} m_3\right)^2 \dots\dots} \quad (2)$$

The elemental components used in the presented work must be considered to evaluate experimental uncertainty. The obtained uncertainty for instruments of temperature measurement, solar radiation, velocity, and distillate yield were ±0.056 °C, ±5.77 W/m^2, ±0.05 m/s, and 0.5 ml respectively. The uncertainties associated with performance parameters of solar still i.e., energy efficiency and exergy efficiency, based on input parameters, are experimentally measured as ±2.08% and ±0.06%, respectively.

3. Mathematical formulation

The mathematical modeling encompasses energy, exergy, economic, and environmental analyses that characterize the overall performance of various configurations. The mathematical modeling was conducted based on specific assumptions, considering the control volume as the basin water of the solar still which are given as,

- The system operates under quasi-steady conditions over each time interval.
- Heat losses through side walls and bottom are negligible due to insulation.
- Vapor leakage is negligible (airtight system).
- Thermophysical properties of water are temperature-dependent but uniform within the control volume.
- The temperature gradient between basin water and vapor is negligible.
- Kinetic and potential exergy changes are neglected.

The transient energy balance for basin water of solar still is expressed as Eqn. 3:

$$I(t)\alpha_b A_b = m_w c_p \frac{dT_w}{dt} + Q_{evap} + Q_{conv} + Q_{rad} \quad (3)$$

3.1. *Energy efficiency*

The thermal energy efficiency for different Solar Stills arrangements was determined from Eqn. 4.

$$\eta_{energy} = \frac{\sum m_w \times L}{\sum I_{t(s)} \times A_s} \quad (4)$$

Productivity of pure water from solar stills in kg/m^2, which is calculated from Eqn. 5 [41], and $\sum m_w$ is the total amount of distillate per day.

$$m_w = \frac{h_{ev,wgi} \times (T_w - T_{gi})}{L} \quad (5)$$

Latent Heat of Evaporation of fresh water at temperature T_w, was determined from Eqn. 6 [41, 14].

$$L = 3161500 - (2407.41 * T_w) \text{ J/kg} \quad (6)$$

The evaporative heat transfer coefficient from water to inner glass, i.e., $h_{ev,w\text{-}gi}$ was calculated from Dunkel relations from Eqn. 7 [41, 14].

$$h_{ev,\,w\text{-}gi} = 0.016273 \times h_{cw} \times \left(\frac{P_w - P_{gi}}{T_w - T_{gi}}\right) \quad (7)$$

The heat transfer coefficient from the convection mode of heat transfer i.e., h_{cw} was determined using Eqn. 8 [41, 16].

$$h_{cw\text{-}gi} = 0.884\left[(Tw - Tgi) + \frac{(Pw - Pgi)\,(Tw + 273.15)}{268900 - Pw}\right]^{\frac{1}{3}} \tag{8}$$

The two important parameters P_w and P_{gi} were calculated using Eqn. 9 and 10 [41, 14].

$$P_w = exp\left[25.317 - \left(\frac{5144}{Tw + 273}\right)\right] \tag{9}$$

$$P_{gi} = exp\left[25.317 - \left(\frac{5144}{Tgi + 273}\right)\right] \tag{10}$$

3.2. Exergy efficiency

Exergy, in simple terms used to define the greatest amount of usable energy that can be used from a system before the system reaches the dead state (i.e., changes in kinetic, potential energy becomes zero, temperature and pressure of system reduces to surrounding atmosphere.) It plays a crucial role in improving the SS performance. Its definition is fraction of output exergy (i.e., exergy of water evaporation in SS) to input exergy (i.e., exergy of sun's radiation intensity).

The exergy efficiency for different solar stills arrangements was computed as given in Eqn. 11 [41, 14].

$$\eta_{exergy} = \frac{\sum \text{Exergy}_{out}}{\sum \text{Exergy}_{in}} \tag{11}$$

Exergy output and exergy input for all different arrangements were evaluated from Eqn. 12 and 13, respectively.

Whereas;

$$\sum Exergy_{out} = \sum Exergy_{evap} = m_w \times L \times \left[1 - \left(\frac{Ta + 273}{Tw + 273}\right)\right] \tag{12}$$

$$\sum Exergy_{in} = \sum Exergy_{sun} = A_s \times \sum I_{t(s)} \times \left[1 - \left(\frac{4}{3} \times \left(\frac{T_a + 273}{T_s}\right) + \frac{1}{3} \times \left(\frac{T_a + 273}{T_s}\right)^4\right)\right] \tag{13}$$

3.3. Economic analysis

Economic analysis is yet another crucial criterion determining whether the existing system is cost-effective, compatible, and sustainable when compared to a typical working system.

The different parameters involved for economic analysis for different arrangements of solar stills were calculated using Eqn. 14-22 [41, 14].

$$\text{FAC} = CRF \times CC \tag{14}$$

And

$$\text{Capital Recovery Factor (CRF)} = \frac{i(i+1)^n}{(i+1)^n - 1} \tag{15}$$

$$\text{ASV} = \text{SFF} \times \text{SV} \tag{16}$$

$$\text{Sinking fund factor (SFF)} = \frac{i}{(i+1)^n - 1} \tag{17}$$

And

$$\text{Salvage value (SV)} = 0.2 \times \text{CC} \tag{18}$$

$$\text{AMC} = 0.10 \times \text{FAC} \tag{19}$$

Now,

$$\text{Total annual cost (TAC)} = \text{FAC} + \text{AMC} - \text{ASV} \tag{20}$$

Finally,

$$\text{Cost Per Litre (CPL)} = \frac{\text{TAC}}{\text{Pd}} \tag{21}$$

Pay-back Period estimates the time period needed to recover the capital cost invested in designing any system. It is also an important parameter regarding determining the feasibility of system. Smaller is the pay-back period of system, higher is the feasibility and vice-versa.

The pay-back period for a current solar desalination system is calculated using Eqn. 22 [16,41].

$$PBP=\frac{\ln\left(\frac{m\times SP}{m\times SP-(CC\times AMC)\times i}\right)}{\ln(1+i)} \tag{22}$$

3.4. Environmental analysis

Promoting the use of solar-assisted desalination technology helps to lower carbon emissions in the atmosphere. This study's environmental analysis aims to forecast how much CO_2 emissions will be reduced as a result of using this technology, considering baseline technology as grid-powered water production, representing conventional electricity-based desalination or water supply.

3.4.1. CO_2 emissions and mitigation

An average power-producing station releases 980g CO_2/kW of CO_2 into the atmosphere when it generates electricity. Nevertheless, taking into account 40% losses from distribution and transmission and about 20% losses from inefficient domestic devices, the total CO_2 per kWh is calculated to be 2kg. Thus, the annual CO_2 emission and CO_2 mitigation by solar distillers can be calculated from the Eqn. 23, 24, 25 [49].

$$CO_2 \text{ emission per year} = \frac{E_{in}\times 2}{n} \tag{23}$$

$$CO_2 \text{ emission in total life span (tons)} = \frac{E_{in}\times 2}{1000} \tag{24}$$

The amount of CO_2 mitigated over the life span of the system can be expressed as

$$CO_2 \text{ mitigate (tons)}\left(\vartheta_{co_2}\right)=\frac{E_{en,out}\times n\times 2}{1000} \tag{25}$$

3.5. Enviro-economic analysis

This analysis evaluates the impact of environmental policy on the economy and economic activities on the environment to balance environmental sustainability and economic growth. In addition, this analysis evaluates the carbon credit earned in terms of CO_2 emissions and also promotes in minimizing the carbon emissions to the lowest possible extent.

The net CO_2 mitigation from all different arrangements of solar stills can be evaluated from Eqn. 26 [50].

$$\text{Net } CO_2 \text{ mitigate (tons)} = \left(\frac{\left(\left(E_{en,out}\times n\right)-E_{in}\right)\times 2}{1000}\right) \tag{26}$$

3.5.1. Carbon credit earned

It allows the emission of carbon dioxide (CO_2) or an equivalent quantity of another greenhouse gas (GHG) for the organizations that have carbon credit validation. Here, one credit simply refers to one ton of CO_2 or other greenhouse gas emissions. And, for 1 credit, the trade price is \$14.5. Therefore, the net carbon credit acquired over lifetime from all different arrangements was calculated from Eqn. 27 [50].

Carbon Credit Earned (CCE) = Carbon Credit × Monetary value per ton.

$$CCE\ (USD) = \left(\frac{\left(\left(E_{en,out}\times n\right)-E_{in}\right)\times 2}{1000}\right)\times USD/tco_2 \tag{27}$$

Embodied energy is defined as the energy used at every stage of production. These phases include resource extraction and processing, manufacturing, transportation, and product distribution; they do not include the energy needed to operate and dispose of building materials.

4. Results and discussions

This section outlines the half-hourly fluctuations of environmental parameters, including solar intensity, wind speed, and ambient temperature, over the next 24 hours during daytime in October. Furthermore, variations in environmental parameters throughout the day lead to fluctuations in the temperature of the inner glass, basin water, and NFs across all configurations, namely setup 1, setup 2, setup 3, setup 4, setup 5, and setup 6, which were conducted six consecutive days. This section additionally encompasses the variations in energy, exergy efficiency, and yield concerning daytime across various configurations of SS. The economic and environmental analyses have been conducted for various solar still configurations.

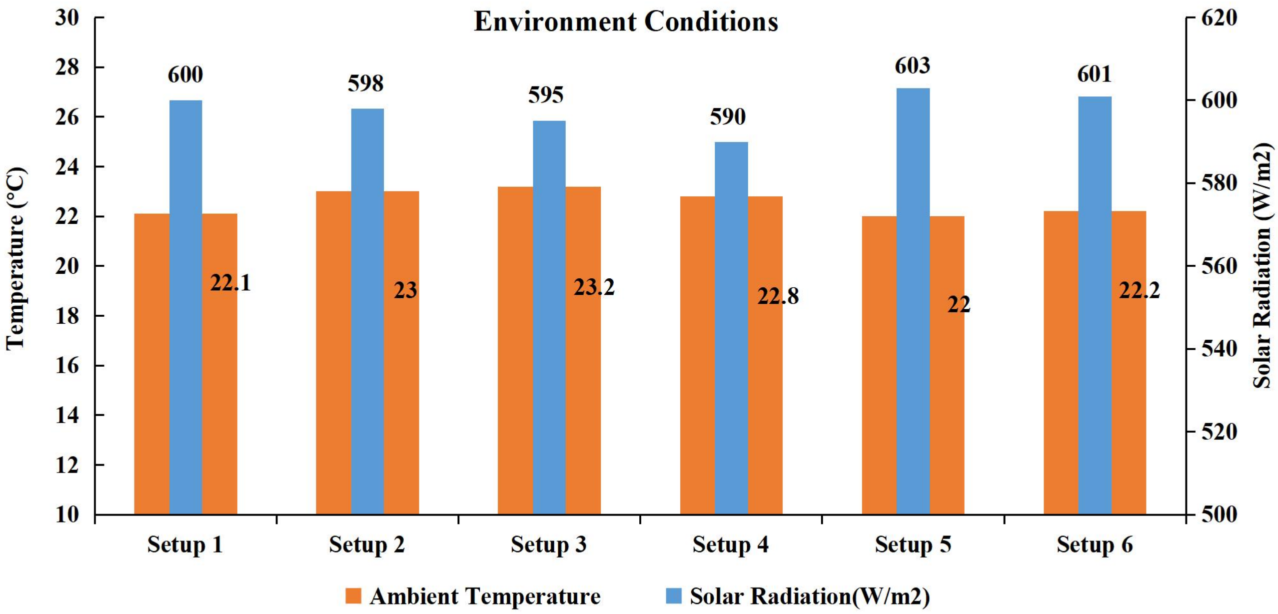

Figure 4. Variation of average solar intensity and ambient temperature with daytime for all setups.

Figure 4 shows the average values of solar radiation and ambient temperature for all six consecutive days for performing experiments in all six setups, i.e., setup 1, setup 2, setup 3, setup 4, setup 5, and setup 6. It is found that there is very small variation in solar radiation and ambient temperature for all six days with the values as, 597±10 W/m^2 and 22.5±0.5°C, respectively. Therefore, it is clear that there are approximately similar environmental conditions for all the setups and further can be compared based on their performance parameters.

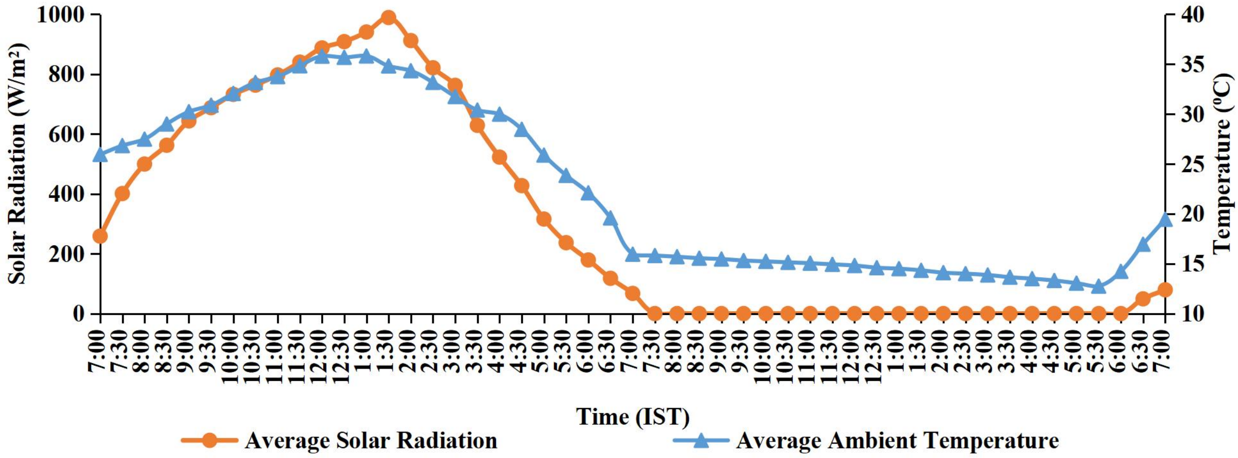

Figure 5. Variation of average solar intensity and ambient temperature with daytime.

Figure 5 shows the variation of the average solar intensity and ambient temperature with daytime for all six days of experiments performed in all the setups, which indicates that the sun's radiation intensity increases as the sun rises from morning at 7:00 a.m. and reaches a maximum value of 989 W/m^2 around 1:30 p.m., and then it starts decreasing continuously, while at the next day, it starts rising from 6:00 a.m. In addition, the variation in ambient temperature occurs similarly to that of solar intensity, as both are directly related to each other. The average values of solar radiation and ambient temperature for the days of the experiments performed in all the setups vary approximately between 500-600 W/m^2 and 21-24°C, respectively.

4.1. Temperature variations at various sections of solar still

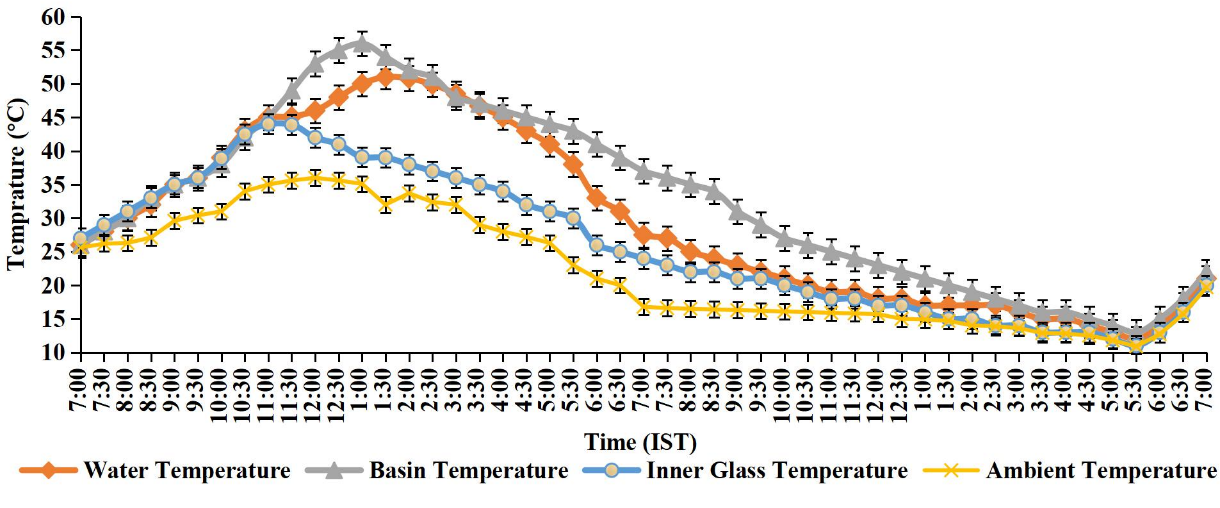

Figure 6. Temperature variations with time for setup 1.

Figure 6 presents the temperature variations of the inner glass, basin, water, and ambient conditions for Setup-1. These temperatures increase with solar intensity, peaking around 1:00 p.m., followed by a subsequent decline. Although solar radiation has decreased, internal temperatures continue to be elevated due to efficient insulation. The temperature of the inner glass begins to decline after 11:00 a.m., signaling the start of condensation and yield collection. The highest recorded temperatures for water, inner glass, and basin are 51°C, 44°C, and 56°C, respectively, alongside peak ambient temperature and solar intensity of 36°C and 855 W/m^2.

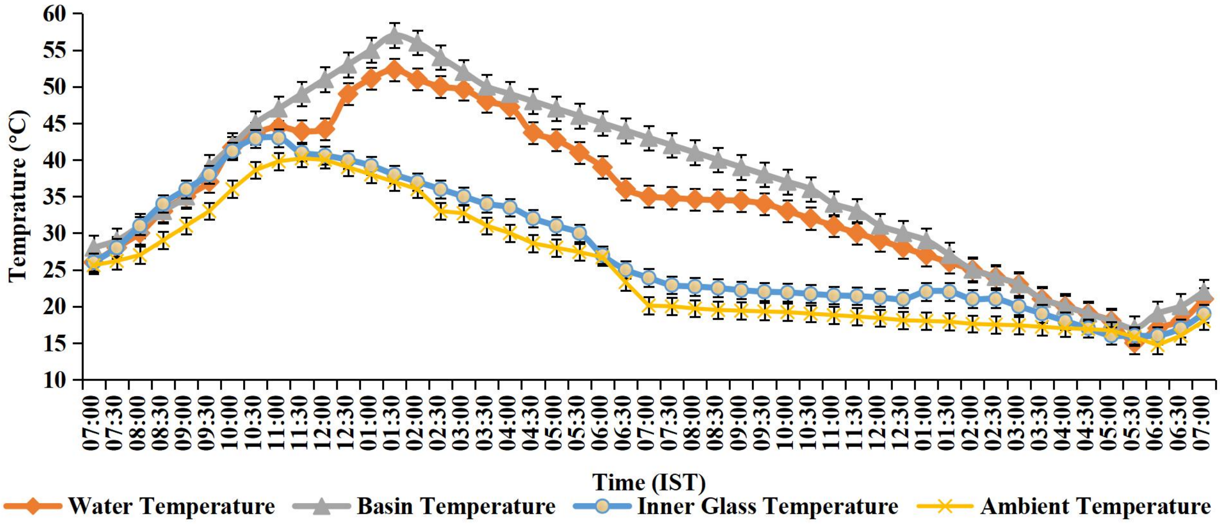

Figure 7. Temperature variations with time for setup 2.

Figure 7 illustrates the fluctuations in temperatures at the inner glass, basin, water, and ambient conditions for setup 2. The temperature variation mirrors that observed in setup 1. The maximum recorded temperatures for water, inner glass, and basin are 52.3°C, 43°C, and 57°C, respectively. The maximum recorded ambient temperature and solar intensity are 35°C and 1000 W/m2, respectively, while the average values are 23.4°C and 534.4 W/m2, respectively. The inner glass temperature begins to decrease at 11:00 a.m., coinciding with the onset of water condensation after this time. The basin temperature and water temperature for setup 2 exceed those of setup 1, indicating improved performance of the stepped solar still (setup 2) relative to the conventional solar still (setup 1).

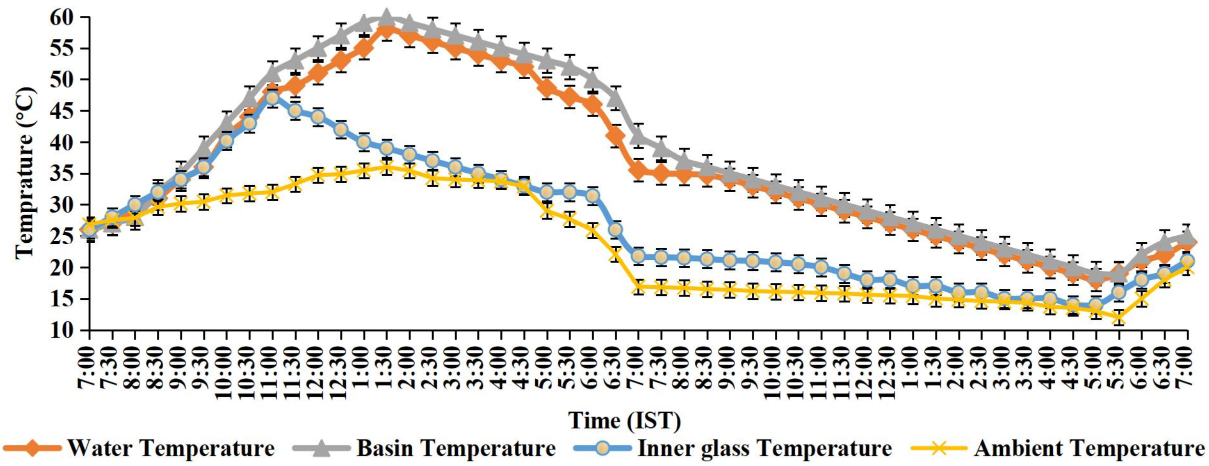

Figure 8. Temperature variations with time for setup 3.

Figure 8 illustrates the temperature variations observed at the inner glass, basin, water, and ambient conditions for setup 3. The temperature variation parallels that observed in setups 1 and 2. The maximum recorded temperatures for water, inner glass, and basin are 58°C, 47°C, and 60°C, respectively. The recorded peak ambient temperature and solar intensity are 36°C and 1031 W/m2, respectively, while the average values are 23.2°C and 602.5 W/m2, respectively. The inner glass temperature begins to decrease at 11:00 a.m., coinciding with the onset of water condensation after this time. The basin temperature and water temperature for setup 3 exceed those of setups 1 and 2, indicating improved performance of the stepped solar still utilizing silver-based nanofluid compared to the conventional solar still (setup 1) and the stepped solar still (setup 2).

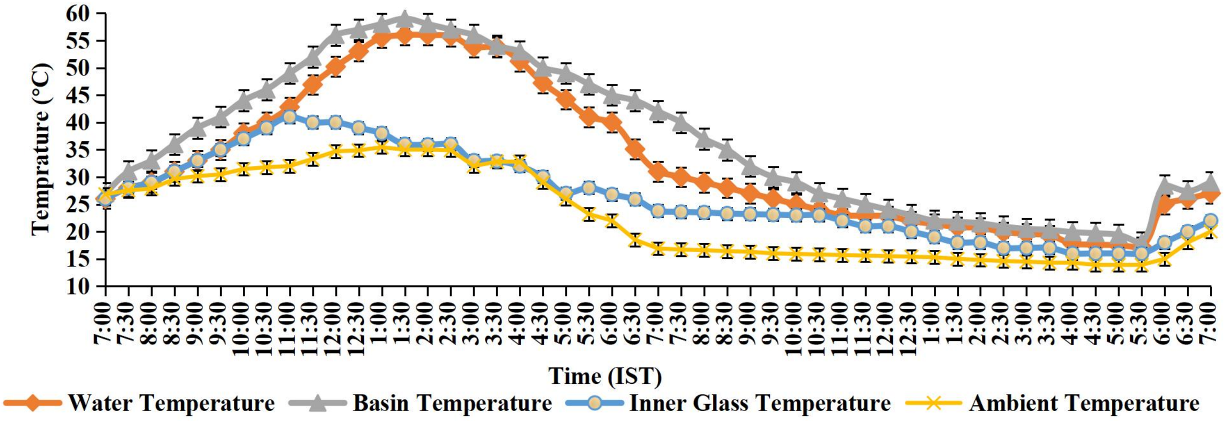

Figure 9. Temperature variations with time for setup 4.

Figure 9 illustrates the temperature variations at the inner glass, basin, water, and ambient conditions for setup 4. The temperature variation parallels that observed in setups 1, 2, and 3. The maximum recorded temperatures for water, inner glass, and basin are 56, 41, and 59°C, respectively. The recorded peak ambient temperature and solar intensity are 35.4°C and 970 W/m2, respectively, while the average values are 22.8°C and 497.7 W/m2, respectively. The inner glass temperature begins to decrease at 11:00 a.m., coinciding with the onset of water condensation after this time.

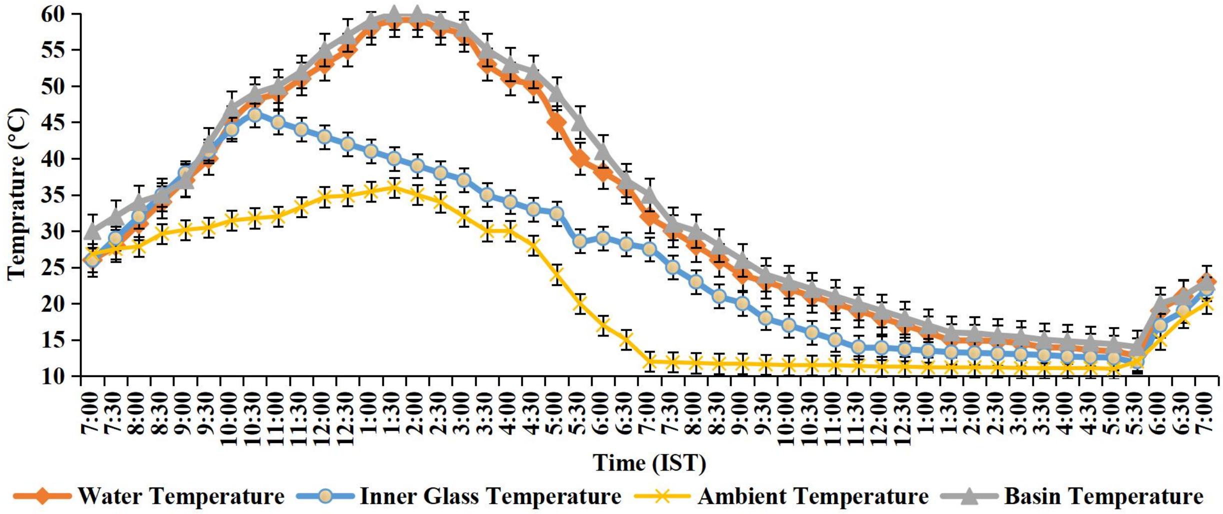

Figure 10. Temperature variations with time for setup 5.

Figure 10 illustrates the temperature variations observed at the inner glass, basin, water, and ambient conditions for setup 5. The temperature variation mirrors that observed in setups 1, 2, 3, and 4. The maximum recorded temperatures for water, inner glass, and basin are 59°C, 46°C, and 60°C, respectively. The maximum recorded ambient temperature and solar intensity are 36°C and 978 W/m², respectively, while the average values are 20.6°C and 540.6 W/m², respectively. The inner glass temperature begins to decrease at 10:30 a.m., coinciding with the onset of water condensation. This suggests that this setup initiates water condensation earlier than other configurations. The basin and water temperatures for setup 5 exceed those of setups 1, 2, 3, and 4, despite lower average ambient temperature and solar radiation. This suggests improved performance of the stepped solar still utilizing a higher concentration of silver-based nanofluid compared to the other setups.

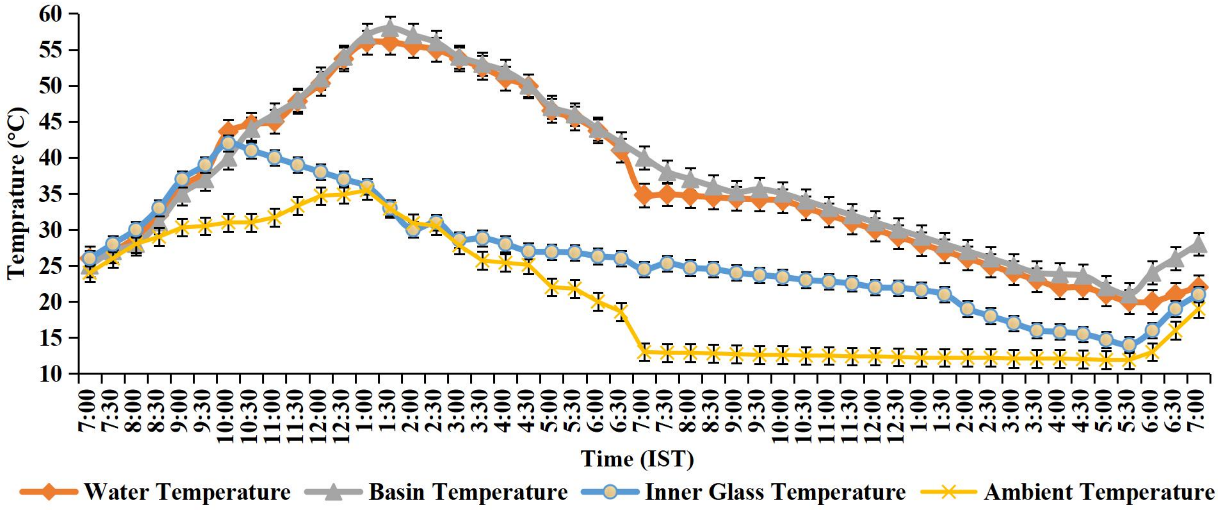

Figure 11. Temperature variations with time for setup 6.

Figure 11 illustrates the variations in inner glass, basin, water, and ambient temperatures for setup 6. The temperature variation mirrors that observed in setups 1, 2, 3, 4, and 5. The maximum recorded temperatures of water, inner glass, and basin are 56°C, 42°C, and 58°C, respectively. The recorded peak ambient temperature and solar intensity are 35.4°C and 980 W/m2, respectively, while the average values are 20.4°C and 578.5 W/m2, respectively. The inner glass temperature begins to decrease at 10:00 a.m., coinciding with the onset of water condensation. This suggests that this setup initiates water condensation earlier than the other setups. The basin temperature and water temperature for setup 6 are lower than those for setup 5 due to the higher concentration of silver in the nanofluid, which absorbs more heat. Nonetheless, setup 6 produces a higher yield due to the increased heat availability during non-sunshine hours in comparison to the other setups. This demonstrates the improved performance of the stepped solar still utilizing a silver-based nanofluid at a concentration of 0.07% in comparison to alternative configurations.

4.2. Energy efficiency

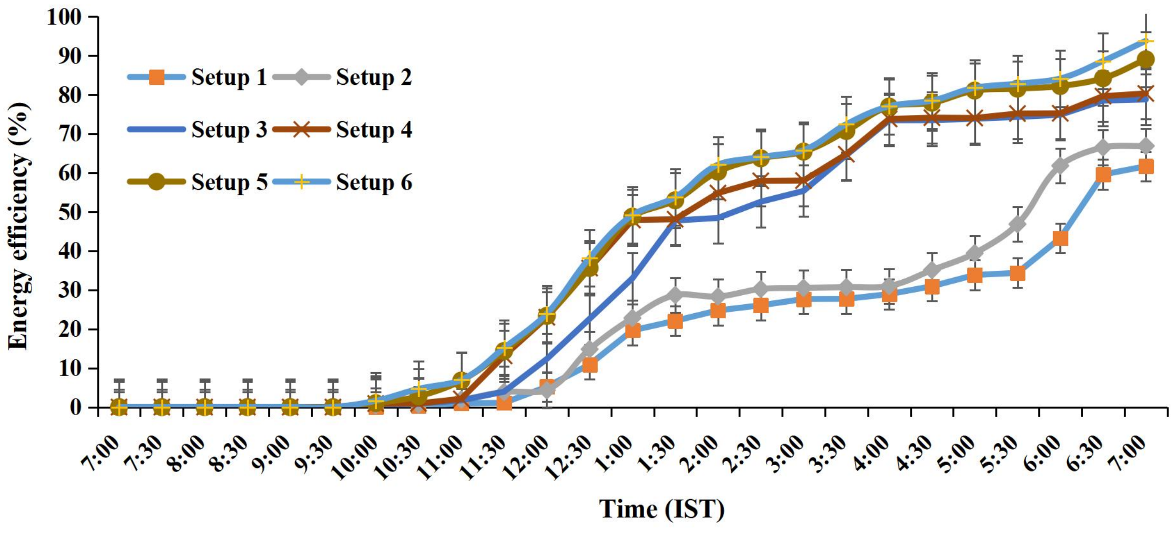

Figure 12. Energy efficiency variation for all different setups with daytime.

Figure 12 illustrates the changes in energy efficiency across various configurations. The efficiency of all setups improves throughout the day, from 10:00 a.m. to 7:00 p.m. The initial rise in energy efficiency, occurring from approximately 10:00 a.m. to 2:00 p.m., results from an increase in solar radiation intensity. This intensification leads to greater heat absorption by basin water, thereby accelerating the evaporation rate. Furthermore, between 2:00 p.m. and 4:00 p.m., as well as after 4:00 p.m., the intensity of solar radiation gradually diminishes, leading to a sudden decrease post 4:00 p.m. Despite this, energy efficiency improves across all setups. The enhancement in energy efficiency is attributed to effective insulation, which facilitates the retention of absorbed heat energy, thereby enabling water evaporation even during non-sunlight hours. The redesign of modified stills, specifically the implementation of a stepped slope, has enhanced energy efficiency by facilitating a quicker collection of condensed yield compared to traditional solar stills, in which the condensed yield must traverse the full length of the glass cover's slope. The average energy efficiency values for setups 1 through 6 are 24.15%, 28.66%, 35.69%, 45.81%, 49.42%, 53.59%, and 54.94%, respectively. This suggests that setup 6 exhibits superior energy efficiency relative to the other setups.

The maximum energy efficiency is observed in a modified still featuring a stepped slope single basin with silver nanofluid at a concentration of 0.07%, designated as setup 6. This is followed by setup 5, with conventional solar stills, identified as setup 1, exhibiting the minimum efficiency. The observed variations result from enhanced heat transfer attributed to the increased thermal conductivity provided by silver nanoparticles, leading to accelerated evaporation compared to conventional solar stills. The significant disparity in energy efficiency between solar stills utilizing silver-based nanofluid and those without underscores the effectiveness of silver nanoparticles in solar distillation applications.

4.3. Exergy efficiency

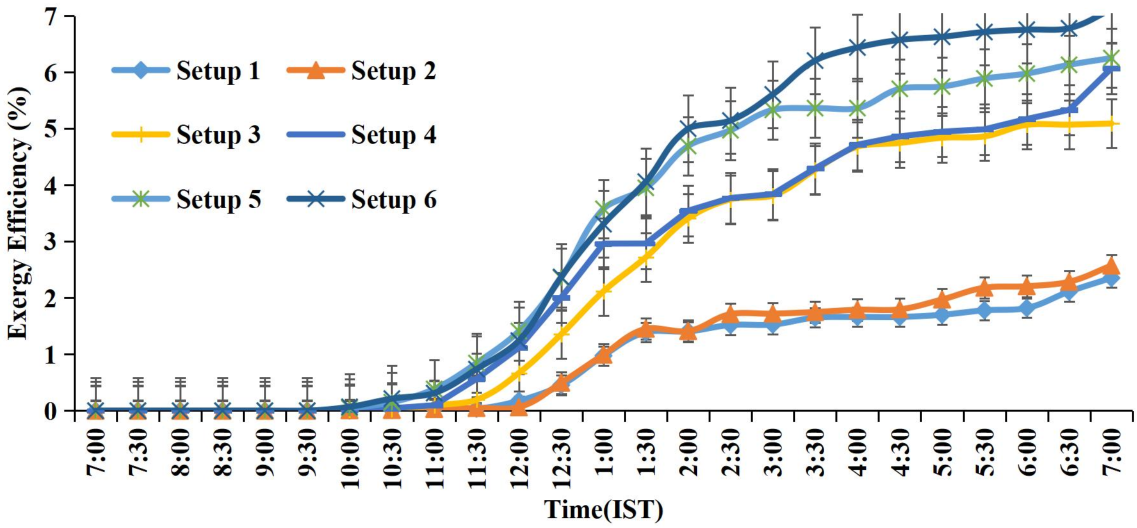

Figure 13. Exergy efficiency variation for all different setups with daytime.

Figure 13 illustrates the changes in exergy efficiency across various setups throughout the daytime, specifically from 10:00 a.m. to 7:00 p.m. The variation in exergy efficiency closely resembles that of energy efficiency. Exergy efficiency reaches its peak in modified stills featuring a stepped slope single basin with a silver nanofluid concentration of 0.07% (setup 6), followed by a modified still with a 0.05% concentration (setup 5), and subsequently decreases, with conventional solar stills exhibiting the lowest efficiency. The peak exergy efficiency at 0.07% concentrations is associated with enhanced high heat transfer, resulting from increased thermal conductivity in basin water with silver nanofluid, thereby facilitating more rapid evaporation compared to conventional solar stills. The abrupt increase in exergy efficiency observed after 4:00 p.m. across all configurations can be attributed to a significant reduction in solar radiation intensity, as well as the effective insulation and the utilization of silver nanofluids for sensible heat storage. The heat energy retained within the system facilitates water evaporation and yield production during non-sunshine hours, thereby enhancing exergy efficiency. The average exergy efficiency values for setups 1, 2, 3, 4, 5, and 6 are 1.17%, 1.29%, 2.21%, 2.99%, 3.22%, 3.90%, and 4.28%, respectively. This demonstrates that setup 6 exhibits superior exergy efficiency relative to the other setups.

4.4. Yield productivity

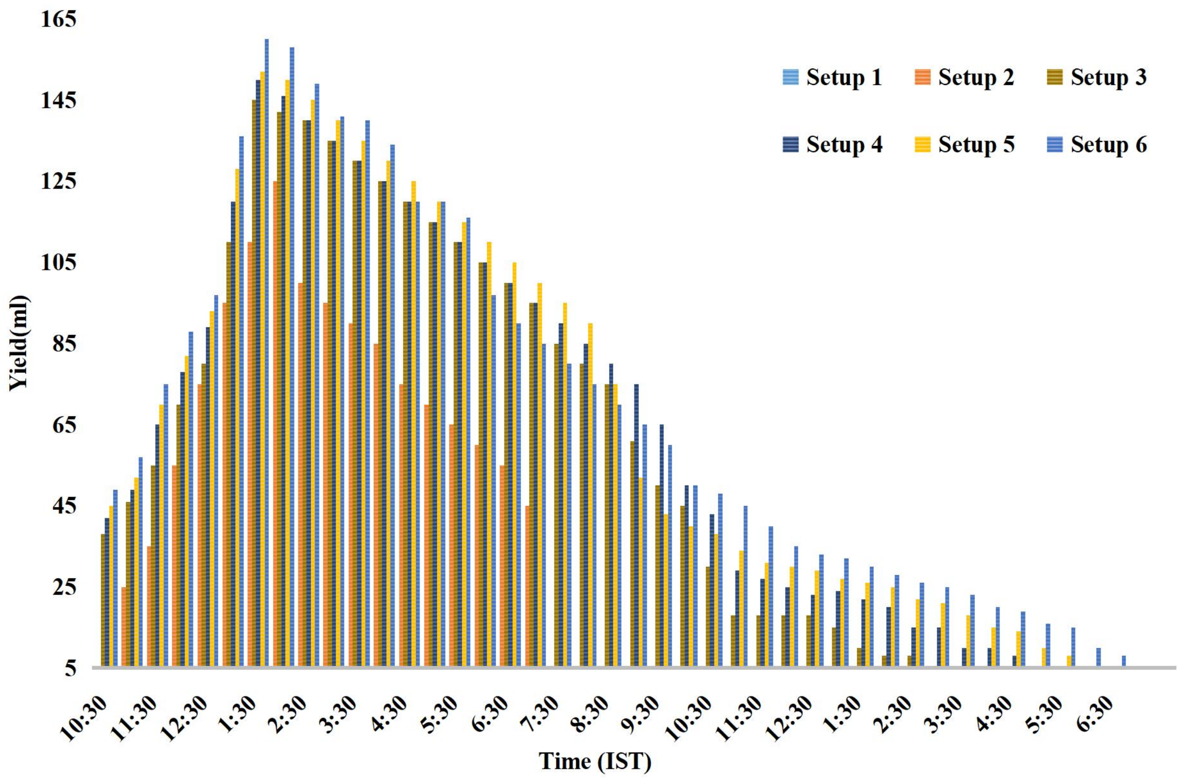

Figure 14. Yield productivity variation for all different setups with time.

Figure 14 illustrates the variation in half-hourly yield productivity across various setups over a 24-hour period. At the outset, yield productivity was recorded as zero across all setups from 6:00 a.m. to 10:00 a.m., attributable to the thermal inertia of the basin water. Upon overcoming thermal inertia, the basin water begins to evaporate, resulting in yield production. Figure 13 indicates that during a specific time period, the maximum yield productivity was observed in a modified still featuring a stepped slope single basin with silver nanofluids at a concentration of 0.07% (setup 6). This was followed in descending order by setups 5, 4, 3, and 2, with the conventional solar still (setup 1) exhibiting the minimum productivity. The highest yield is observed in setup 6, followed by setup 5, attributed to enhanced thermal conductivity in the basin water resulting from the incorporation of silver nanofluid within a copper cylindrical structure. This configuration facilitates an increased heat transfer rate, consequently elevating the evaporation rate. The total yields collected over a 24-hour period for setups 1, 2, 3, 4, 5, and 6 are 1260 ml, 1750 ml, 2410 ml, 2630 ml, 2745 ml, and 2810 ml, respectively. These volumes correspond to yield productions of 1.26 kg/m², 1.75 kg/m², 2.41 kg/m², 2.63 kg/m², 2.745 kg/m², and 2.81 kg/m², respectively. The stepped solar still utilizing 0.07% silver nanofluid generates 2.23 times the water output compared to the conventional solar still.

4.5. Economic analysis

The economic analysis is done to ensure whether the designed or modified setups are economically feasible within the reach of the common man. Here, the capital cost of solar still setups includes the cost incurred in GI sheets, glass cover, PVC pipes, copper cylinders, silver nanoparticles, fabrication, transportation, deionized water, labor costs, etc which is further given in Table 4. Assuming an interest rate of 8% for the life span of 10 years with working hours of 300 days each year for all different setups, the various economic parameters were calculated using Eqn. 12-19. All the economic parameters for all setups are given in Table 5. It is clear that setup 6 has a 45.16% shorter payback period compared to setup 1, while the cost of water produced from setup 6 is 44.26% lower compared to the water produced from setup 1.

Table 2. Various fabrication (items) cost of the setups.

Item	Unit prize ($)	Setup 1	Setup 2	Setup 3	Setup 4	Setup 5	Setup 6
GI Sheet	4.82/sheet	38	38	38	38	38	38
Copper	18.07/sheet		3	3	3	3	3
PVC	4.82/pipe	2	3	3	3	3	3
Glass (3mm thick)	26/m^2	28	28	28	28	28	28
Black Paint	6.61/liters	3	3	3	3	3	3
Labour + Transportation	—	8	9	9	9	9	9
Deionized Water	—			0.7	0.7	0.7	0.7
Magnetic Stirrer	—			3	3	3	3
Ag Nanoparticles	2.29/gram	0	0	3	5.6	8.4	12.3
Total ($)		**79**	**84**	**90.7**	**93.3**	**96.1**	**100**

Table 3. Various economic factors with the corresponding value for all the setups.

Parameters	Values					
	Setup-1	Setup-2	Setup-3	Setup-4	Setup-5	Setup-6
Interest Rate (*i*)	8 %	8 %	8 %	8 %	8 %	8 %
Life span (*n*) (Years)	10	10	10	10	10	10
Capital cost (CC) ($)	79	84.75	90.7	93	96	100.3
Capital Recovery Factor (CRF)	0.149	0.149	0.149	0.149	0.149	0.149
First annual cost (FAC) ($)	11.771	12.628	13.516	13.857	14.304	14.945
Annual Maintenance Cost ($)	1.177	1.263	1.351	1.386	1.430	1.494
Sinking Fund Factor	0.0690	0.0690	0.0690	0.0690	0.0690	0.0690
Salvage value ($)	15.8	16.95	18.14	18.6	19.2	20.06
Annual Salvage value ($)	1.091	1.170	1.252	1.284	1.325	1.385

Total Annual cost (TAC) ($)	11.857	12.720	13.616	13.959	14.409	15.054
Production Periods (Days)	300	300	300	300	300	300
Production Per Day (kg/m^2)	1.260	1.750	2.410	2.630	2.745	2.810
Cost per liter (CPL) ($)	0.03138	0.02423	0.01883	0.01770	0.01750	0.01749
Payback period (PP) Months	11.433	8.757	6.76	6.345	6.274	6.269

4.6. Environmental analysis

In order to properly evaluate the environmental characteristics of an experimental setup, it is essential to take into account the embodied energy, which refers to the energy that is generated during the manufacturing process of the material that is utilized in each component. Table 6 lists the embodied energies of each solar still's components, which shows that the stepped solar still with nanofluids (169.75 kWh) has approximately 15% greater embodied energy compared to the conventional solar still (142.99 kWh). Although the quantity of nanoparticles used is relatively small, their high energy intensity may influence the net environmental benefit. It is now explicitly stated that the overall sustainability of the proposed system depends on balancing these upstream impacts against the operational CO_2 mitigation achieved during its lifetime.

Table 4. Embodied energy of individual components and different setups used in all setups.

Setup	**Item**	**Materials**	**Total weight (kg)**	**Energy Density (MJ/kg)**	**(kWh/kg)**	**Embodied Energy E_{in} (kWh)**
Setup 1	Frame/Structure	GI Sheet	11	13.9	3.86	42.46
	Pipe	PVC	0.5	70	19.44	9.72
	Inclined glass cover	Glass	9	31.5	8.75	78.75
	Black Paint					
			0.6	90.4	25.11	15.06
						Total E_{in} = 142.99
Setup 2	Frame/Structure	GI Sheet	11	13.9	3.86	42.46
	Pipe	PVC	0.8	70	19.44	9.72
	Black Paint		0.6	90.4	25.11	15.06
	Stepped glass cover	Glass	9	31.5	8.75	78.75
	Copper cylinder	Copper	1.2	70.6	19.61	23.53
						Total E_{in} = 169.52
Setup 3	Frame/Structure	GI Sheet	11	13.9	3.86	42.46
	Copper cylinder	Copper	1.2	70.6	19.61	23.53
	Pipe	PVC	0.8	70	19.44	9.72
	Black Paint		0.6	90.4	25.11	15.06
	Stepped glass cover	Glass	9	31.5	8.75	78.75
	Nano-Particle					
	(0.01%concentration)	Ag	0.00226	55	14.85	0.033
						Total E_{in} = 169.55
Setup 4	Frame/Structure	GI Sheet	11	13.9	3.86	42.46
	Copper cylinder	Copper	1.2	70.6	19.61	23.53
	Pipe	PVC	0.8	70	19.44	9.72
	Black Paint		0.6	90.4	25.11	15.06

	Stepped glass cover	Glass	9	31.5	8.75	78.75
	Nano-Particle (0.03% concentration)	Ag	0.00678	55	14.85	0.100
						Total E_{in} = 169.62
Setup 5	Frame/Structure	GI Sheet	11	13.9	3.86	42.46
	Copper cylinder	Copper	1.2	70.6	19.61	23.53
	Pipe	PVC	0.8	70	19.44	9.72
	Black Paint		0.6	90.4	25.11	15.06
	Stepped glass cover	Glass	9	31.5	8.75	78.75
	Nano-Particle (0.05% concentration)	Ag	0.0113	55	14.85	0.167
						Total E_{in} = 169.68
Setup 6	Frame/Structure	GI Sheet	11	13.9	3.86	42.46
	Copper cylinder	Copper	1.2	70.6	19.61	23.53
	Pipe	PVC	0.8	70	19.44	9.72
	Black Paint		0.6	90.4	25.11	15.06
	Stepped glass cover	Glass	9	31.5	8.75	78.75
	Nano-Particle (0.07% concentration)	Ag	0.0158	55	14.85	0.234
						Total E_{in} = 169.75

Table 5. Environmental parameters for each setup over a period of 15 years.

Setup	E_{in} (kWh)	$E_{en,out}$ (kWh)	Annual CO_2 emitted (in tons) over entire life span	CO_2 mitigated (in tons) over entire life span	Net CO_2 reduction (tons)	Earned Carbon credit ($)
Setup 1	171.126	263.6667	0.3422	7.910	7.5677	109.732
Setup 2	193.806	303.2167	0.3876	9.322	8.7088	126.278
Setup 3	294.786	453.8837	0.5895	13.673	13.0269	188.890
Setup 4	361.611	521.6837	0.7232	15.763	14.927	216.445
Setup 5	361.611	542.4000	0.7232	16.272	15.5487	225.457
Setup 6	428.436	555.5837	0.8568	16.611	15.8106	229.254

Utilizing renewable energy-based solar-powered devices greatly lowers carbon emissions, which pose a serious threat to the environment. To measure the rate of carbon emissions and the system's potential decrease, environmental analysis is carried out. The average CO_2 emission during the production of energy from grid connected power plants is roughly 980 g CO_2/kWh [50]. Nevertheless, the effective emission factor rises to about 2 kg CO_2/kWh when end-use inefficiencies and transmission and distribution losses are taken into account. Since, carbon dioxide is one of the main greenhouse gases causing global warming, it is widely acknowledged as a crucial indicator of environmental impact. By substituting renewable solar energy for fossil fuel-based energy, solar stills reduce CO_2 emissions.

Table 7 delineates the environmental performance of all solar still configurations over a 15-year duration, utilizing embodied energy values from Table 6 to estimate parameters including annual CO_2 emissions, total

CO_2 mitigation, net CO_2 reduction, and accrued carbon credits. The findings demonstrate that Setup 6 displays superior environmental performance, attaining the highest CO_2 mitigation (16.611 tons) and net CO_2 reduction (15.8106 tons), exceeding those of Setup 1 (7.910 tons and 7.5677 tons, respectively) by over 100%. Furthermore, Setup 6 generates the highest carbon credit revenue of $229.254, indicating both ecological and financial advantages. The upward trend from Setup 1 to Setup 6

Table 6. Comparative table for various performance parameters of solar stills with previous works.

S N.	Type of Solar Still	Modifications	Novelity	Yield (kg/m²/day)	Energy Efficiency (%)	Exergy Efficiency (%)	Reference
1	Single-Slope Solar Still	Hybrid thermal energy storage system with paraffin wax and black gravel	Combination of latent (PCM) and sensible heat storage	2.95	32.00	2.50	**[51]**
2	Single-Slope Solar Still	Soya wax as PCM	Use of eco-friendly, biodegradable PCM	3.1	30.51	2.10	**[52]**
3	Single-Slope Solar Still	Various water depths (3 to 6 cm)	Optimization of basin water depth	2.68	30.52	2.20	**[53]**
4	Stepped basin tubular solar still	tubular solar still	Integration of stepped basin with tubular geometry	2.58	24.59	2.80	**[54]**
5	Single-Slope Passive Solar Still	Various water depths (1, 2, 3 cm)	analysis of shallow water depths	2.75	30.00	2.80	**[55]**
6	Modified Solar Still	Graphite and copper oxide nanofluids	Enhancement of thermal conductivity and solar absorption using hybrid nanofluids	2.90	41.18	4.32	**[56]**
7	Single-slope solar still	Composite heat storage material	Development of composite PCM	2.98	44.20	3.00	**[57]**
8	**Stepped slope single basin Solar Still**	**Silver-based Nanofluid having 0.07% concentration filled in copper cylinder**	Synergistic effect of high thermal conductivity Ag nanofluid and copper cylinder	**2.81**	**49.75**	**3.46**	**Present study**

Table 8 depicts the comparison of various performance parameters of solar stills used in previous studies with the present study. From this table, it is found that the energy efficiency and exergy efficiency of stepped solar still used in present study are found to be greater than that of previous studies. Also, a higher yield of production is found as compared to the others. This is the indication of feasibility of silver-based nanofluid to be used in stepped solar still for enhancing the performance parameters.

5. Conclusions

This experimental study has conducted for energy, exergy, economic, and environmental analyses for six distinct configurations at Gorakhpur location, namely, conventional single slope CSS (**setup 1**), modified stills with stepped wise slope single with single basin (MSWSSSB) (**setup 2**), MSWSSSB filled with silver nanofluid inside copper cylindrical shape copper pipe prepared at a volume concentration of 0.01% (**setup 3**), MSWSSSB filled with silver nanofluid inside copper cylindrical shape copper pipe having at volume concentration of 0.03% (**setup 4**), MSWSSSB filled with silver nanofluid inside cylindrical shape copper pipe having at volume concentration of 0.05% (**setup 5**), MSWSSSB filled with silver nanofluid inside cylindrical shape copper pipe having at volume concentration of 0.07% (**setup 6**).

The following things have been observed from the experimental study,

- The energy and exergy efficiency of all configurations improve as solar radiation intensity increases. However, the energy and exergy efficiency of the conventional setup, i.e., Setup 1, is comparatively lower than that of other setups. This increase in energy and exergy efficiency for modified setups accounts for the reason that the modified setup with a stepped slope has increased the rate of collecting the condensed water, i.e., yield output. Further, the use of nanofluid in a cylindrical copper tube has increased the thermal conductivity of basin water, leading to higher heat transfer and hence maintaining a greater temperature difference between the basin water and the inner glass.
- The average exergy efficiency was investigated as highest for Setup 6, 3.46%, followed by Setup 5, 3.29%, followed by Setup 4, 2.50%, followed by Setup 3, 2.56% followed by Setup 2, 1.92% and lowest for Setup 1, having 1.48%.
- Similarly, the average energy efficiency was investigated as highest for Setup 6, i.e., 49.75% followed by Setup 5, 45% followed by Setup 4, 44% followed by Setup 3, 41% followed by Setup 2, 39% and lowest for Setup 1, 31%
- The yield productivity obtained daily was highest from setup 6, 2.81 kg/m^2, followed by Setup 5, 2.745 kg/m^2 followed by Setup 4, 2.63 kg/m^2 followed by Setup 3, 2.41 kg/m^2 followed by Setup 2, 1.75 kg/m^2 and lowest yield productivity from setup 1 is 1.26 kg/m^2.
- The price of each litre of distillate produced was minimum from setup 6 (0.0174$) and maximum from the conventional setup (0.0313$).
- The payback time for setup 1 is 11.43 months, setup 2 is 8.75 months, setup 3 is 6.48 months, setup 4 is 6.34 months, setup 5 is 6.27 months, and setup 6 is 6.26 months.
- The highest net CO_2 mitigation came from setup 6, 17.55 tons, followed by setup 5, 15.22 tons, followed by setup 4, 13.84 tons, followed by setup 3, 12.02 tons, followed by setup 2, 9.33 tons, and the lowest net CO_2 mitigation from the conventional setup, 7.24 tons.

This study concludes that the performance of SSSS can be enhanced by using silver-based nanofluids at 0.07% concentration. In future, this study can further be proceeded by different modifications in the design of solar stills, such as a stepped slope of inner glass with a stepped basin, along with the use of different sensible heat storage, i.e., utilizing different hybrid nanofluids having high thermal conductivity at different concentrations, and also utilizing different phase change materials having high latent heat storage at a suitable melting temperature can also be investigated for performance enhancement.

Abbreviations

AMC	**Annual Maintenance Cost**
ASV	Annual Salvage Value
CCE	Carbon Credit Earned (USD)
CPL	Cost Per Litre of Distilled Water
CRF	Capital Recovery Factor
FAC	Fixed Annual Cost
IST	Indian Standard Time
NEPCM	Nano-Enhanced Phase Change Material
NF	Nanofluid
PBP	Pay-Back Period
SFF	Sinking Fund Factor
SP	Selling Price
SV	Salvage Value
TAC	Total Annual Cost
Nomenclature	
m	Yield Productivity (kg)
T_w	Water Temperature (°C)
T_{gi}	Temperature at Inner Glass (°C)
$h_{ev,w-gi}$	Water to Inner Glass heat transfer coefficient (Evaporative type) ($W/m^2 \cdot K$)
h_{cw-gi}	Water to Inner Glass heat transfer coefficient (Convective type) ($W/m^2 \cdot K$)
P_w	Vaporisation Pressure (Temperature of water)
P_{gi}	Vaporisation Pressure (Temperature of glass)
η_{energy}	Thermal Energy Efficiency (%)
η_{exergy}	Exergy Efficiency (%)
$Exergy_{out}$	Output Exergy (J)
$Exergy_{in}$	Input Exergy (J)
T_s	Sun's Temperature (K), 5700 K
Q_{cond}	Conductive heat transfer through basin water
Q_{conv}	Covective heat transfer through basin water
Q_{rad}	Radiative heat transfer through basin water
T_a	Ambient Temperature (°C)
E_{in}	Embodied Energy (kWh/year)
$E_{en,out}$	Output Energy from Solar Desalination System (kWh/year)
i	Annual Interest Rate
n	Life Span (years)
φ	Volume percent concentration
M	Mass of nanoparticles
a	accuracy of an instrument

u	uncertainty
m	independent variables
U	resulting uncertainties
L	Latent Heat of Evaporation
P_d	Annual distillate produced from Solar stills operated for 300 clear sunny days
ϱ	Density of Nanoparticle

Availability of Data and Materials: Data will be made available on reasonable request.

Author Contributions: Vikas Kumar conceptualized and designed the research framework; carried out the experimental and computational work; performed the data analysis and formal analysis; and prepared the initial draft of the manuscript. Dheerandra Singh provided critical guidance on the analytical methods and interpretation of results ; supervised the project; and managed resources. He also reviewed and edited the manuscript. Virendra Kumar reviewed and edited the manuscript and contributed to validation of the findings. All authors contributed to editorial changes in the manuscript. All authors have read and approved the final manuscript. All authors have participated sufficiently in the work and agree to be accountable for all aspects of the work.

Acknowledgment: The authors are very thankful to the Head of the Department, Mechanical Engineering Department and Chemical Engineering Department, MMMUT Gorakhpur, for providing the research facilities and nanofluid preparation to complete the experimental work.

Funding: The authors declare that no funds, grants, or other support were received during the preparation of this manuscript.

Conflict of Interest: The authors declare no conflict of interest.

Declaration of AI and AI-assisted Technologies in the Writing Process: The authors have not used AI tools anywhere of the manuscript.

References

1. Bhargva, M.; Yadav, A. Productivity augmentation of single-slope solar still using evacuated tubes, heat exchanger, internal reflectors and external condenser. *Energy Sources, Part A: Recovery, Utilization, and Environmental Effects* 2019, 46(1), 2646-2666. https://doi.org/10.1080/15567036.2019.1691291.
2. Abujazar, M.S.S.; Fatihah, S.; Rakmi, A.R.; Shahrom, M.Z. The effects of design parameters on productivity performance of a solar still for seawater desalination: A review. *Desalination* 2016, 385, 178-193. https://doi.org/10.1016/j.desal.2016.02.025.
3. Al-Mezeini, S.S.; Siddiqui, M.A.; Shariq, M.; Althagafi, T.M.; Ahmed, I.A.; Asif, M.; Alsufyani, S.J.; Ahamed, M.B.N.; Elamin, K.M.A.; Alaghaz, A.N.; Gomaa, M.M. Design and experimental studies on a single-slope solar still for water desalination. Water 2023, 15, 704. https://doi.org/10.3390/w15040704.
4. Attia, M.E.H.; Kabeel, A.E.; Abdelgaied, M.; Essa, F.A.; Omara, Z.M. Enhancement of hemispherical solar still productivity using iron, zinc and copper trays. *Solar Energy* 2021, 216, 295-302. https://doi.org/10.1016/j.solener.2021.01.038.
5. Alwan, N.T.; Shcheklein, S.E.; Ali, O.M.; Majeed, M.H.; Agyekum, E.B. Experimental and theoretical investigations of a modified single-slope solar still with an external solar water heater. *Sustainability* 2021, 13(22), 12414. https://doi.org/10.3390/su132212414.
6. Gholizadeh, M.; Farzi, A. Performance improvement of the single slope solar still using sand. *Journal of Solar Energy*

Research 2020, 5(4), 560-567. 10.22059/jser.2020.302120.1152.

7. Chaichan, M.T.; Kazem, H.A.; Al-Waeli, A.H.A.; Mohammed, S.A.; Omara, Z.M.; Sopian, K. Performance enhancement of solar distillation system works in harsh weather conditions: An experimental study. *Thermal Science and Engineering Progress* 2023, 43, 101981. https://doi.org/10.1016/j.tsep.2023.101981.
8. Al-harahsheh, M.; Al-Fahed, S.; Al-Salaymeh, A. Performance evaluation of a solar still integrated with solar collector and phase change material (Sodium Thiosulfate Pentahydrate) Experimental study. *Desalination* 2020, 491, 114534. https://doi.org/10.1016/j.desal.2018.09.020.
9. Ramzy, K.; Abdelgaleel, M.; Kabeel, A.E.; Mosalam, H. Performance of a single slope solar still using different porous absorbing materials: An experimental approach. *Environmental Science and Pollution Research* 2023, 30(28), 72398-72414. https://doi.org/10.1007/s11356-023-27465-5.
10. Alasiri, A.; Shanmugan, S. The role of Mn_2O_3-Cu NanoPCM in aluminum cans for enhancing thermal performance and freshwater yield of M-shaped basin solar desalination system: An experimental analysis. *Separation and Purification Technology* 2025, 377, 134267. https://doi.org/10.1016/j.seppur.2025.134267.
11. Vijayakumar, R.; Karthick, A. Performance enhancement of a double slope solar still using Glauber salt and graphene oxide-based PCM composites. *Separation and Purification Technology* 2025, 378, 134584. https://doi.org/10.1016/j.seppur.2025.134584.
12. Shajahan, M.I.; Narayana, D.R.; RadhaKrishnan, N.S.; Michael, J.J. Evaluation of efficiency of double slope solar still and drinking water yield using silver nanoparticle mixed with phase change material. *Energy Sources, Part A: Recovery, Utilization, and Environmental Effects* 2022, 44(4), 8679-8693. https://doi.org/10.1080/15567036.2022.2120572.
13. Karthikeyan, J.; Selvaraj, P.; Nagaraj, G. Day and night yield performance analysis of solar still for saline water using energetic materials with thermocol insulation. *Materials Today: Proceedings* 2020, 33, 4848-4851. https://doi.org/10.1016/j.matpr.2020.08.395.
14. Gupta, S.; Solanki, S.C. Enhancing the performance of double-slope solar still using nano-enhanced eutectic phase change materials and steel wool fibre as wick material. *Journal of the Brazilian Society of Mechanical Sciences and Engineering* 2024, 46(5), 274. https://doi.org/10.1007/s40430-024-04853-7.
15. Hafs, H.; Ansari, O.; Bah, A. Performance evaluation of a production system of solar desalination by using rectangular channels with PCM at different seasons. *Acta Ecologica Sinica* 2023, 43(4), 690-700. https://doi.org/10.1016/j.chnaes.2022.09.001.
16. Suraparaju, S.K.; Sampathkumar, A.; Natarajan, S.K. Experimental and economic analysis of energy storage-based single-slope solar still with hollow-finned absorber basin. *Heat Transfer* 2021, 50(6), 5516-5537. https://doi.org/10.1002/htj.22136.
17. Poonia, S.; Singh, A.K.; Jain, D. Performance evaluation of PCM based solar concentrator type desalination device. Materials Today: Proceedings 2022, 62, 5194-5200. https://doi.org/10.1016/j.matpr.2022.02.637.
18. Kumaravel, S.; Nagaraj, M.; Bharathiraja, G. Study on the performance of single slope solar still using marble stone as energy storage material. In *Proceedings of the 5th International Conference on Smart Systems and Inventive Technology (ICSSIT)*; 2023; pp. 278-283. https://doi.org/10.1109/ICSSIT55814.2023.10060919.
19. Suraparaju, S.K.; Natarajan, S.K. Performance analysis of single slope solar desalination setup with natural fiber. *Desalination and Water Treatment* 2020, 193, 64-71. https://doi.org/10.5004/dwt.2020.25679.
20. Kumbhar, S.V. Double slope solar still distillate output data set for conventional still and still with or without reflectors and PCM using high TDS water samples. *Data in Brief* 2019, 24, 103852. https://doi.org/10.1016/j.dib.2019.103852.
21. Kouravand, A.; Shabestari, S.T.; Zirak, N.; Kasaeian, G.; Fereidooni, L.; Kasaeian, A. Thermal management strategies for a portable double slope solar still with energy storage: An experimental study for enhancing the performance. *Next Energy* 2025, 8, 100244. https://doi.org/10.1016/j.nxener.2025.100244.

22. El-Sebaii, A.A.; Al-Ghamdi, A.A.; Al-Hazmi, F.S.; Faidah, A.S. Thermal performance of a single basin solar still with PCM as a storage medium. Applied Energy 2009, 86(7-8), 1187-1195. https://doi.org/10.1016/j.apenergy.2008.10.014.
23. Tuly, S.S.; Rahman, M.S.; Sarker, M.R.I.; Beg, R.A. Combined influence of fin, phase change material, wick, and external condenser on the thermal performance of a double slope solar still. *Journal of Cleaner Production* 2021, 287, 125458. https://doi.org/10.1016/j.jclepro.2020.125458.
24. Faegh, M.; Shafii, M.B. Experimental investigation of a solar still equipped with an external heat storage system using phase change materials and heat pipes. *Desalination* 2017, 409, 128-135. https://doi.org/10.1016/j.desal.2017.01.023.
25. Mousa, H.; Gujarathi, A.M. Modeling and analysis the productivity of solar desalination units with phase change materials. *Renewable Energy* 2016, 95, 225-232. http://dx.doi.org/10.1016/j.renene.2016.04.013.
26. Damene, D.; Kemerchou, I.; Djouahi, A. Advanced heat storage integration strategies for high-efficiency solar water heating applications. *Journal of Ovonic Research* 2026, *22*(1), 79-90. https://doi.org/10.15251/JOR.2026.221.79
27. Abdullah, A.S.; Alawee, W.H.; Mohammed, S.A.; Majdi, A.; Omara, Z.M.; Younes, M.M. Utilizing a single slope solar still with copper heating coil, external condenser, phase change material, along with internal and external reflectors-Experimental study. *Journal of Energy Storage* 2023, 63, 106899. https://doi.org/10.1016/j.est.2023.106899.
28. Benghanem, M.; Attia, M.E.H.; Abdelgaied, M.; Harby, K.; Bedairi, B.H. A multifaceted experimental approach for enhancing solar distiller productivity: Nano-coated heat coil integrated with solar nanofluid collector, nano-coated absorber, nano-enhanced PCM, reflectors, and PV panels. *International Communications in Heat and Mass Transfer* 2025, 167, 109401. https://doi.org/10.1016/j.icheatmasstransfer.2025.109401.
29. Sathyamurthy, R. Silver (Ag) based nanoparticles in paraffin wax as thermal energy storage for stepped solar still – An experimental approach. *Solar Energy* 2023, 262, 111808. https://doi.org/10.1016/j.solener.2023.111808.
30. Chaichan, M.T.; Kazem, H.A.; Al-Ghezi, M.K.S.; Al-Waeli, A.H.A.; Ali, A.J.; Sopian, K.; Kadhum, A.A.H.; Isahak, W.N.R.W.; Takriff, M.S.; Al-Amiery, A.A. Effect of different preparation parameters on the stability and thermal conductivity of MWCNT-based nanofluid used for photovoltaic/thermal cooling. *Sustainability* 2023, 15(9), 7642. https://doi.org/10.3390/su15097642.
31. Kumar, M.; Patel, S.K.; Mishra, V.; Singh, D.; Giri, B.S.; Singh, D. Performance analysis of modified solar still with parabolic reflector and nanofluids. *Journal of the Taiwan Institute of Chemical Engineers* 2025, 166, 105651. https://doi.org/10.1016/j.jtice.2024.105651.
32. Sahu, R.; Tiwari, A.C. Experimental investigation for performance enhancement of single slope solar still using nanofluids under winter conditions. *Desalination and Water Treatment* 2023, 304, 1–11. https://doi.org/10.5004/dwt.2023.29799.
33. Singh, D.; Singh, S.; Singh, D.; Kushwaha, J.; Mishra, V.; Patel, S.K.; Tewari, S.; Giri, B.S. Sustainable pathways for solar desalination using nanofluids: a critical review. *Environmental Research* 2024, 241, 117654-117654. https://doi.org/10.1016/j.envres.2023.117654.
34. Gajbhiye, T.; Shelare, S.; Aglawe, K. Current and future challenges of nanomaterials in solar energy desalination systems in last decade. *Transdisciplinary Journal of Engineering & Science* 2022, 13, 187-20. https://doi.org/10.22545/2022/00217.
35. Isravel, S.; Karunamurthy, K. A review of solar thermal desalination using nanotechnology. *Materials Today: Proceedings* 2023, 84, 74–82. https://doi.org/10.1016/j.matpr.2023.05.084.
36. Parsa, S.M.; Rahbar, A.; Koleini, M.H.; Aberoumand, S.; Afrand, M.; Amidpour, M. A renewable energy-driven thermoelectric-utilized solar still with external condenser loaded by silver/nanofluid for simultaneously water disinfection and desalination. *Desalination* 2020, 480, 114354. https://doi.org/10.1016/j.desal.2020.114354.
37. Zakaria, M.; Sharaky, A.M.; Al-Sherbini, A.S.; Bassyouni, M.; Rezakazemi, M.; Elhenawy, Y. Water desalination using solar thermal collectors enhanced by nanofluids. *Chemical Engineering & Technology* 2022, 45(1), 15-25.

https://doi.org/10.1002/ceat.202100339.

38. Sathish, T.; Saravanan, R.; Giri, J.; Ghodhbani, R.; Sabeur, H.; Abdullah, M.; Anderson, A. Enhancing solar thermal desalination with MWCNT/TiO2 nanofluids for sustainable water solutions. *Case Studies in Thermal Engineering* 2025, 74, 106797. https://doi.org/10.1016/j.csite.2025.106797.
39. Patel, P.; Modi, K.V.; Patel, S.K. Experimental study of mono and hybrid nanofluids on square pyramid solar still. *Environmental Science and Pollution Research* 2025, 32(2), 693-724. https://doi.org/10.1007/s11356-024-35619-2.
40. El-Gazar, E.F.; Zahra, W.K.; Hassan, H.; Rabia, S.I. Fractional modeling for enhancing the thermal performance of conventional solar still using hybrid nanofluid: Energy and exergy analysis. *Desalination* 2021, 503, 114847. https://doi:10.1016/j.desal.2020.114847.
41. Sai, G.; Anna, V.R.; Swapna, K.; Prasad, M.V.K.S.; Ch, R.P.; Krishna, B.C.; Mandhala, V.N.; Madhav, B.T.P.; Praveenkumar, S.; Saleh, S.M.; Rao, M.C.; Shanmugan, S. Evaluating the effects of sugarcane juice-mediated ZnO nanofluids on solar light activation for enhancing double-slope solar still performance. *Applied Materials Today* 2025, 42, 102542. https://doi.org/10.1016/j.apmt.2024.102542.
42. Kandasamy, V.K.; Jaganathan, S.; Dhairiyasamy, R.; Rajendran, S. Optimizing the efficiency of solar thermal collectors and studying the effect of particle concentration and stability using nanofluidic analysis. *Energy & Environment* 2023, 34(5), 1564-1591. https://doi.org/10.1177/0958305X231183687.
43. Rasaiah, N.; Eugine, R.; Manickam, R. Efficiency, productivity and economic analysis of polystyrene foam–insulated conventional and modified double-slope solar still using nanofluids. *Environmental Science and Pollution Research* 2025, 32, 12713–12742. https://doi.org/10.1007/s11356-025-36469-2.
44. Prasad, A.R.; Harshith, V.; Harish, R.; Venkatesh, I.; Prakash, M.A.; Ravishankar, S. Investigating single sloped (SSl) and square pyramid (SPy) solar stills using phase changing material (PCM). *Materials Today: Proceedings* 2023; https://doi.org/10.1016/j.matpr.2023.08.334.
45. Harby, K.; Elazab, M.A.; Amer, T.S.; Almetwally, E.M. Productivity enhancement of hemispherical solar distillers using spiral tube absorber coated with Cu-NPs integrated with recycled porous filler materials and nanofluid-spiral tube collector powered by PV system. *Separation and Purification Technology* 2026, 394, 137336. https://doi.org/10.1016/j.seppur.2026.137336
46. Elango, T.; Hemarana, K.; Kalidasa Murugavel, K.; Sasidhar, M. Effect of renewable energy and water nanofluids in improving the performance of passive solar distillation. *Journal of Water Chemistry and Technology* 2026, 48, 94-106. https://doi.org/10.3103/S1063455X26010029.
47. Said, Z.; Sajid, M.H.; Alim, M.A.; Saidur, R.; Rahim, N.A. Experimental investigation of the thermophysical properties of Al_2O_3-nanofluid and its effect on a flat plate solar collector. *International Communications in Heat and Mass Transfer* 2013, 48, 99-107. https://doi.org/10.1016/j.icheatmasstransfer.2013.09.005.
48. Mahian, O.; Kianifar, A.; Kalogirou, S.A.; Pop, I.; Wongwises, S. A review of the applications of nanofluids in solar energy. *International Journal of Heat and Mass Transfer* 2013, 57 (2), 582–594. https://doi.org/10.1016/j.ijheatmasstransfer.2012.10.037.
49. Aghakhani, S.; Kavehfarsani, M.; Pordanjani, A.H.; Afrand, M. Energy and exergoeconomic analysis of solar stills integrated with thermoelectric technology: A case study on environmental and economic sustainability. *Renewable Energy* 2025, 239, 121989. https://doi.org/10.1016/j.renene.2024.121989
50. Kumar, S.; Ahmad, A.; Irshad, K.; Prakash, O.; Kausher, R.; Hasnain, S.M.; Paramasivam, P.; Ayanie, A.G.; Giri, J. Energy-exergy and environ-economic (4E) analysis of heat storage-based single-slope solar stills integrated with solar air heater. *PLoS One* 2025, 20(1), 0314036. https://doi.org/10.1371/journal.pone.0314036.
51. Saad, F.O.; Mankai, S.; Madiouli, J.; Chemkhi, S.; Shigidi, I.; Khan, M.I. Effect of phase change materials melting temperature on improving single slope solar still productivity. *Journal of Energy Storage* 2024, 97, 112927. https://doi.org/10.1016/j.est.2024.112927.

52. Mayilsamy, Y.; Natarajan, S.; Balakrishnan, D.; Ramalingam, S.K.; Kalidass, A.K. Experimental investigation of single slope solar still by varying water depth and with external reflector. *Journal of Studies in Science and Engineering* 2024, 4(1), 75-90. https://doi.org/10.53898/josse2024416.
53. El-Sebaey, M.S.; Hegazy, A.; Essa, F.A. Performance enhancement of a tubular solar still by using stepped basins: An experimental approach. *Journal of Cleaner Production* 2024, 437, 140746. https://doi.org/10.1016/j.jclepro.2024.140746.
54. Khafaji, H.Q.; Wahhab, H.A.; Al-Maliki, W.A.K.; Alobaid, F.; Epple, B. Energy and exergy analysis for single slope passive solar still with different water depth located in Baghdad center. *Applied Sciences* 2022, 12(17), 8561. https://doi.org/10.3390/app12178561.
55. Sharshir, S.W.; Peng, G.; Elsheikh, A.H.; Edreis, E.M.; Eltawil, M.A.; Abdelhamid, T.; Kabeel, A.E.; Zang, J.; Yang, N. Energy and exergy analysis of solar stills with micro/nano particles: A comparative study. *Energy Conversion and Management* 2018, 177, 363-375. https://doi.org/10.1016/j.enconman.2018.09.074.
56. Sampathkumar, A.; Suraparaju, S.K.; Natarajan, S.K. Enhancement of yield in single slope solar still by composite heat storage material-experimental and thermo-economic assessment. *Journal of Solar Energy Engineering* 2023, 145(2), 021005. https://doi.org/10.1115/1.4055100.